

# Static Balancing of Single Loop Reconfigurable Mechanisms

P.D. Robertson



# Static Balancing of Single Loop Reconfigurable Mechanisms

by

P.D. Robertson

to obtain the degree of Master of Science  
at the Delft University of Technology,  
to be defended publicly on Wednesday June 8<sup>th</sup>, 2016 at 1:30 PM.

Student number:	1509845	
Thesis committee:	Prof. dr. ir. J.L. Herder,	TU Delft, supervisor
	Prof. dr. C. -H. Kuo,	NTUST
	Prof. dr. ir. P. Breedveld	TU Delft
	Dr. ir. P. Lambert	TU Delft

An electronic version of this thesis is available at <http://repository.tudelft.nl/>.



# Preface

This graduation project started a few thousand kilometres east of Delft, in Taiwan. The National Taiwan University of Science and Technology was the place for starting the internship that grew to be my graduation. The aim of the placement at NTUST was to prove that a reconfigurable mechanism designed by a former student there could be balanced using a single spring. The mechanism was a rehabilitation device for patients with lower limb weakness and designing a statically balanced mechanism would relieve therapists from having to physically guide the patients in the motions they would have to perform. By finding if this mechanism could be balanced with a single spring, a more convenient prototype of the mechanism could be made.

In this report, the main subject will be Paper 1, the graduation paper. The technological advances are described here. Paper 1 will also talk about other mechanisms that can be statically balanced. These other mechanisms are introduced in Paper 2, the literature review, that suggests that more groups of reconfigurable mechanisms may be balanced using a generalised theory. The rest of this document are the Appendices where you will find preliminary and explanatory work with early sketches of possible solutions. Then descriptions of the methods of validation are presented for the mechanism found in Paper 1. These include the details and full results of the simulation and renderings and the experimental set-up for a physical prototype.

*P.D. Robertson  
Delft, May 2016*



# Contents

<b>1 Graduation Paper</b>	<b>1</b>
<b>2 Review Paper</b>	<b>13</b>
<b>A Preliminary Work</b>	<b>23</b>
A.1 Current Solution by Tseng . . . . .	23
A.2 Static balancing . . . . .	24
A.3 First concept . . . . .	25
<b>B ADAMS</b>	<b>27</b>
B.1 ADAMS Build details . . . . .	27
B.1.1 Spring calculations . . . . .	27
B.1.2 Cable Toolbox . . . . .	29
B.1.3 Motions . . . . .	30
B.1.4 Solver settings . . . . .	30
B.2 Full ADAMS Results . . . . .	31
<b>C Physical Model</b>	<b>33</b>
C.1 Details of the physical model . . . . .	33
C.2 Physical model Solidworks Design . . . . .	36
C.3 Experiment Design . . . . .	37
C.4 Full test results . . . . .	40
C.5 Test Result Processing . . . . .	43
<b>Bibliography</b>	<b>45</b>



1

# Graduation Paper

# The static balancing of single-loop reconfigurable mechanisms

P.D. Robertson, J.L. Herder, C.-H. Kuo

**Abstract**—Reconfigurable mechanisms are a relatively recent contribution to the field of mechanism design and authors have only just been producing real-life applications of these mechanisms. This paper builds on the application of two categories of reconfigurable mechanisms by applying a generalised static balancing theory suggested in a previous review paper [1]. These groups are single loop mechanisms with one degree of freedom per mode, and single loop mechanisms with multiple degrees of freedom per mode. In this paper it is shown that all configurations of the single DoF mechanisms can be balanced using a single spring. The multiple DoF mechanisms can be balanced by balancing each link with respect to the previous link. These balancing strategies are mathematically shown to be valid. The theory is then applied to a reconfigurable rehabilitation mechanism by Tseng et al. [2] of which a simulation and a prototype is made to validate the theory. From the simulation and prototype follows that the single spring balancing of multiple configurations of a single DoF mechanism is possible.



## 1 INTRODUCTION

Since 1996, when K. Wohlhart [3] first coined the term Kinematotropic Mechanism for mechanisms that, numerous authors have contributed to the field of reconfigurable mechanisms, as in mechanisms that can change their topology or mobility while in operation. These early contributions focussed on the analysis and synthesis of this new group in mechanism design. More recently, the focus is increasingly on demonstrating the use of reconfigurable mechanisms in real-world applications [2], [4], [5].

In our literature review [1], we showed that the field of reconfigurable mechanisms can be divided into four categories according to their structure and mobility. These categories are Single-Loop Single degree of freedom, Single-Loop Multiple degrees of freedom, Multiple-Loop Single degrees of freedom and Multiple-Loop Multiple degrees of freedom. The review proposed that of these groups, the Single-Loop mechanisms show promise of having a generalisable static balancing strategy.

This paper further elaborates on these generalised static balancing strategies and demonstrates their application in a number of mechanisms in their respective categories. Of the mechanisms in the single-loop single DoF category, a mechanism by Tseng et al. [2] is taken as a main subject. This mechanism was developed as a rehabilitation device for patients suffering from muscular weakness in their legs. The device is able to balance two of the leg motions the patients are required to perform in rehabilitation therapy. Two springs are used to statically balance the weight of the mechanism and the leg of the patient; one spring for each configuration. In this paper it will be shown that the anticipated balancing theory proposed in our literature review [1] can be incorporated in the design of this balancing mechanism. For the Tseng mechanism, a simulation and a physical model were constructed to prove that the balancing strategy works in a real-world

application.

The other group of mechanisms in the single-loop category were the multiple degree of freedom mechanisms. Two mechanisms were found in this category with similar structure. These devices have a ring shape with multiple revolute joints, the orientation of these joints determines their structural topology. Since no specific applications of the single-loop multiple DoF group have yet been identified, in this paper, the static balancing theory is theoretically proven.

## 2 METHODS

### 2.1 Reconfigurable Mechanisms

#### 2.1.1 Single Loop Mechanisms

As our literature study revealed, some groups of reconfigurable mechanisms are compatible with static balancing. This study showed that single loop reconfigurable mechanisms with one or multiple degrees of freedom in the operation modes can be balanced by general static balancing strategies. The two groups shown to have a generalisable balancing strategy are the single-loop, single degree of freedom and single-loop, multiple degree of freedom mechanisms.

#### 2.1.2 Single DoF mechanisms

The mechanisms described in this group have one degree of freedom in each operation mode. Because of this property, it is possible to balance all configurations of these mechanisms using a single spring. The simplest example of a single-loop single DoF mechanisms comes from an example by Müller who devised an over-constrained mechanism as shown in Fig. 2.

### 2.2 Static Balancing

The most straightforward way to apply static balancing to mechanisms is to use zero free-length springs. This allows

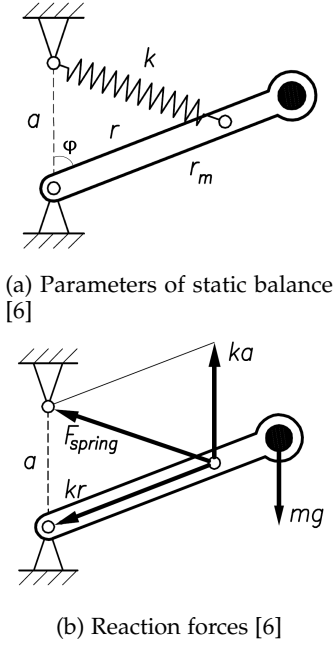


Fig. 1: Balancing of a simple link

the spring to be directly mounted from ground to the link. As depicted in Fig. 1a, there are multiple ways the parameters needed to achieve static balance can be determined. In this paper, a potential energy balance is used. A statically balanced condition is achieved when the sum of the potential energy of the whole system is constant throughout the range of motion of the mechanism. Both the position of the system and the length of the spring are dependent on the same angle. This means we can choose the parameters for a constant potential energy as in 6.

$$l_v = \sqrt{a^2 + r^2 - 2ar \sin(\phi)} \quad (1)$$

Where  $l_v$  is the length of the spring.

$$\mathcal{V}_s = \frac{1}{2}kl_v^2 \quad (2)$$

$$= \frac{1}{2}k(a^2 + r^2) - kar \sin(\phi) \quad (3)$$

Since the calculation assumes zero free-length springs, the length of spring can be taken as the elongation. The potential energy in the spring is shown in Eq. 3.

$$\mathcal{V}_g = mgr_g \sin(\phi) \quad (4)$$

$$\mathcal{V}_{tot} = mgr_g \sin(\phi) + \frac{1}{2}k(a^2 + r^2) - kar \sin(\phi) \quad (5)$$

$$\mathcal{V}_{tot} = (mgr_g - kar) \sin(\phi) + \frac{1}{2}k(a^2 + r^2) \quad (6)$$

From Eq. 6 we can see that if  $mgr_g$  equals  $kar$ , the variable  $\phi$  drops out of the equation and the sum of the potential energy is constant.

### 2.3 Balancing Müller Mechanism

As discussed in the previous section it should be possible to balance Müllers mechanism using zero free-length springs. This static balancing technique can also be applied to the two DoF mechanisms. Figure 2 shows the axes of the joints.

The attachment point of the spring must be in the same vertical plane as the joint. As shown, since the mechanism has two sets of joints, the intersection of the two planes creates a line where the spring can be attached.

Because of the intersecting rotation lines, it can be expected that this mechanism can be balanced using a single spring. This means some parameters have to be the same for both configurations. These parameters are the height of the springs attachment point,  $a$ , and the spring constant,  $k$ . This leaves the connection of the spring to the mechanism as variable to find the parameters to satisfy the potential energy requirement of both configurations. By considering the potential energy of both configurations, the parameters can be found in the relation required for static balancing. The equations for this are as follows. First the length of the spring is defined in Eq 7.

$$l_s(\theta, \phi) = \frac{1}{\sqrt{a^2 + r_1^2 + r_2^2 - 2ar_1 \sin(\theta) - 2ar_2 \sin(\phi)}} \quad (7)$$

The formula for the length of the spring is inserted into the total potential energy of the mechanism.

$$\mathcal{V}_{\theta, \phi} = \frac{1}{2}kl_s^2 + \sum mgh \quad (8)$$

$$\begin{aligned} \mathcal{V}_{\theta, \phi} = & \frac{1}{2}k(a^2 + r_1^2 + r_2^2 - 2ar_1 \sin(\theta) - 2ar_2 \sin(\phi)) \quad (9) \\ & + m_1r_{1g}g \sin(\theta) + m_2r_{2g}g \sin(\phi) \end{aligned}$$

To determine the static balancing conditions, equation that calculates the potential energy for both configurations has to be considered for each mode. The terms are chosen such that the potential energy is no longer dependent on the mechanisms position. Moreover, since this mechanism has two independent configurations, the terms for each mode are reviewed individually. The terms are rearranged by variable terms and the constants for each mode. The first mode in Eq. 10:

$$\begin{aligned} m_1r_{1g}g \sin(\theta) - kar_1 \sin(\theta) = & \\ - \frac{1}{2}k(a^2 + r_1^2 + r_2^2) & \quad (10) \end{aligned}$$

The second mode in Eq. 11:

$$\begin{aligned} m_2r_{2g}g \sin(\phi) - kar_2 \sin(\phi) = & \\ - \frac{1}{2}k(a^2 + r_1^2 + r_2^2) & \quad (11) \end{aligned}$$

To achieve the statically balanced situation we need the potential energy to remain constant in both of the configurations. This is done by choosing the parameters in the relation as in equations 12 and 13.

$$m_1r_{1g}g = kar_1 \quad (12)$$

$$m_2r_{2g}g = kar_2 \quad (13)$$

Additionally, the spring constant has to be equal for both situations so we rewrite the equations above to the relation in equation 14.

$$k = \frac{m_1r_{1g}g}{ar_1} = \frac{m_2r_{2g}g}{ar_2} \quad (14)$$

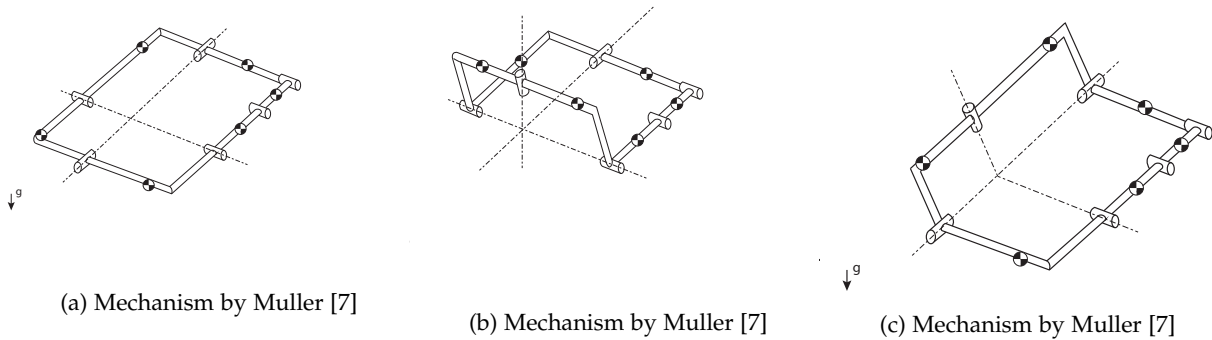


Fig. 2: Mechanisms with different motion orientation

By finding parameters that comply with these equations, a statically balanced mechanism using a zero free-length spring will be obtained.

## 2.4 Balancing Tseng Mechanism

Unlike the mechanism by Müller, in which the attachment point of the spring can be clearly identified. The rotation lines of some mechanisms do not intersect or are parallel. Such is the case in the mechanism used in the lower-limb rehabilitation device designed by Tseng et al. [2] which has two parallel rotation lines as shown in Fig. 3. The mechanism by Tseng et al. is a mechanism designed for people that suffer from a lower limb weakness. These patients are able to activate their muscles but are not strong enough to raise them against gravity [2].

The mechanism is attached to a chair in which the patient will sit. The patient's leg will then be attached to the device and the mechanism will balance the weight of the leg plus the mechanism's own weight. This mechanism is proven to significantly reduce the force required in the patient's muscles to lift their legs. The mechanism has two configurations, one for each motion of the leg. The patient can perform flexion of the hip in the first configuration and extension of the knee in the second configuration. Currently, this mechanism requires one spring to balance each configuration. From our literature review, [1] we know that this mechanism can be placed in the Single Loop single DoF category, which means it can be expected that this mechanism can be also balanced using a single spring.

### 2.4.1 Cable and Pulley Balancing

As described, a zero free-length spring can be used to obtain a statically balanced condition. Fig. 3: Schematic of the mechanism by Tseng et al. [2]. There are, however, some drawbacks to the use of these springs which are expensive and difficult to produce. Zero free-length springs owe their zero free-length property to the larger initial force required to start the elongation of the spring. A viable alternative is to use regular springs in such a way to compensate for the free-length of a spring. For this, a spring and pulley method is used which relies on a cable wound around pulleys to compensate for the free length of the spring.

Applied to Tseng's mechanism [2], the use of a cable

and pulley allows the attachment point of the spring to be shifted to a convenient location. A continuous cable can be mounted from the ground along a pulley to the lower parallelogram so that both motions of the mechanism can be balanced using one spring. Along with the advantage of only requiring one spring, using a cable and pulley also eliminates the need for zero free-length springs [6]. In Fig. 4 the red lines represent the cable that balances both configurations.

When the lower parallelogram is in the vertical position, the whole weight of the mechanism is balanced. When the lower parallelogram is not vertical, only the lower leg masses are balanced.

### 2.4.2 Potential Energy Balance

The design of the balancing of Tseng's mechanism depends on a number of parameters. These parameters are formed by the static balancing conditions and the method of balancing. The static balancing conditions are formulated by summing up the potential energy in the mechanism and choosing the parameters so that the potential energy remains constant. The application of this method is discussed in the following section for two concentrated masses:  $m_{ul}$  for the masses of the upper leg and  $m_{ll}$  for the masses of the lower leg. A more detailed model including all the masses of the patient's leg and the link masses is provided later in the

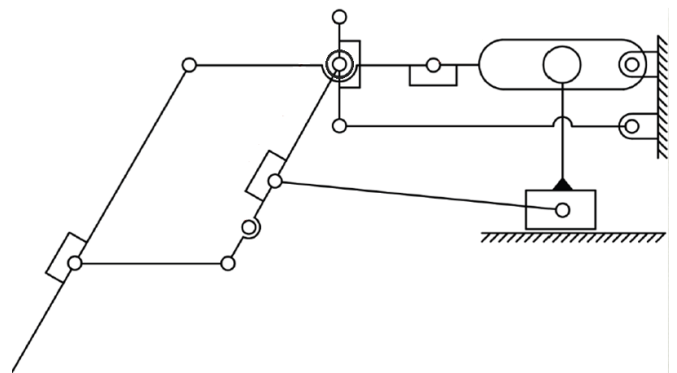


Fig. 3: Schematic of the mechanism by Tseng et al. [2]

paper.

The equations for balancing this mechanism are formulated by considering two independent configurations with overlapping parameters. Because of the nature of the mechanism, the two configuration can not be activated simultaneously so the potential energy of each configuration can be summed independently. The raising of the upper leg, dependent on angle  $\theta$  is called the first configuration. The second configuration is the extension of the lower leg, dependent on angle  $\phi$ . The elongation of the spring is equal to the distance of  $P_1 - P_2$  plus  $P_2 - P_3$ . Using the cosine rule, these distances are:

$$\begin{aligned} P_1 - P_2 &= \sqrt{a_1^2 + r_1^2 - 2a_1r_1 \cos(\frac{\pi}{2} - \theta)} \\ &= \sqrt{a_1^2 + r_1^2 - 2a_1r_1 \sin(\theta)} \end{aligned} \quad (15)$$

$$\begin{aligned} P_2 - P_3 &= \sqrt{a_2^2 + r_2^2 - 2a_2r_2 \cos(\frac{\pi}{2} - \phi)} \\ &= \sqrt{a_2^2 + r_2^2 - 2a_2r_2 \sin(\phi)} \end{aligned} \quad (16)$$

The potential energy of the system is the sum of the gravitational potential energy and the potential energy in the springs. For the mechanism this is summed as in equation 17.

$$\mathcal{V}_{spring} = \frac{1}{2}ku^2 = \frac{1}{2}k((P_1 - P_2)^2 + (P_2 - P_3)^2) \quad (17)$$

$$\mathcal{V}_{gravity} = mgh$$

$$\begin{aligned} \mathcal{V}(\theta, \phi) &= m_1r_1g \sin(\theta) \\ &\quad + m_2(r_3 \sin(\theta) + r_2g \sin(\phi))g \\ &\quad + \frac{1}{2}k(r_1^2 + a_1^2 - 2r_1a_1 \sin(\theta)) \\ &\quad + \frac{1}{2}(r_2^2 + a_2^2 - 2r_2a_2 \sin(\phi)) \end{aligned} \quad (18)$$

$$\begin{aligned} \mathcal{V}(0, \phi) &= m_2r_2g \sin(\phi) - ka_2r_2 \sin(\phi) \\ &\quad + \frac{1}{2}k(a_1^2 + r_1^2 + r_2^2 + a_2^2) \end{aligned} \quad (19)$$

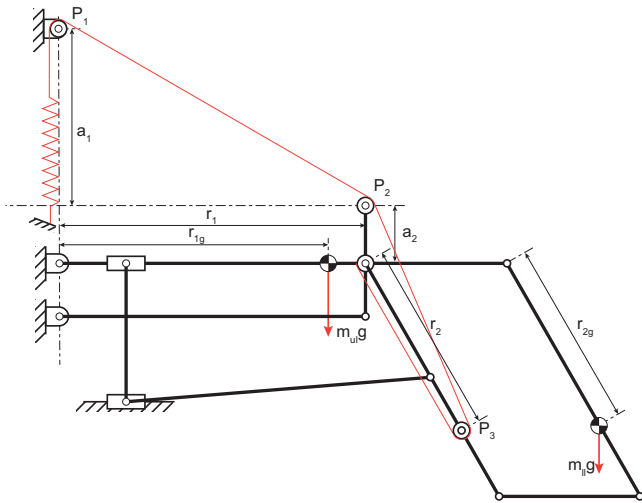


Fig. 4: Single Spring balancing of Tseng mechanism

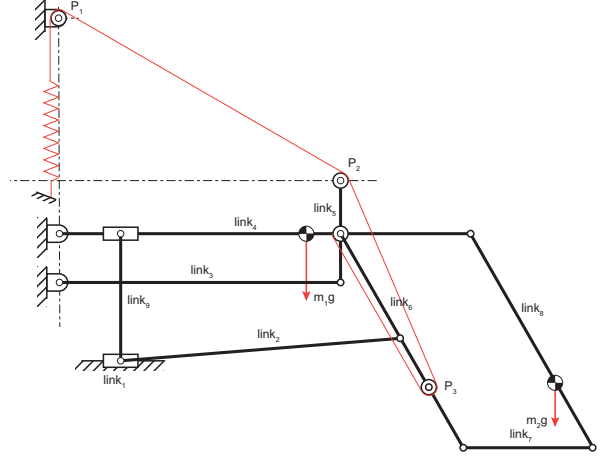


Fig. 5: Link numbers

$$\begin{aligned} \mathcal{V}(\theta, -\pi/2) &= (m_1r_1g + m_2r_3)g \sin(\theta) \\ &\quad - ka_1r_1 \sin(\theta) - m_2r_2g \\ &\quad + ka_2r_2 + \frac{1}{2}k(a_1^2 + r_1^2 + a_2^2 + r_2^2) \end{aligned} \quad (20)$$

Where  $\mathcal{V}$  is the potential energy,  $k$  is the spring stiffness and  $r_3$  is the length of link 4.

Because both configurations operate independently from each other, one angle remains constant while the other can be varied. Equations 18 and 19 show the potential energy in configurations 1 and 2 respectively. The angle  $\phi$  in equation 19 is  $-\pi/2$  and angle  $\theta$  in equation 18 is zero while the other can vary. By moving the constants to the right hand side of the equations we can find the expressions that have to be constant for each of the modes to be balanced:

$$(m_2r_2g - kr_2a_2) \sin(\phi) = \mathcal{C}_1 \quad (21)$$

$$((r_1g m_1 + r_3 m_2)g - kr_1a_1) \sin(\theta) = \mathcal{C}_2 \quad (22)$$

As the cable is attached to the same spring, the spring constants have to be the same. The equations above can

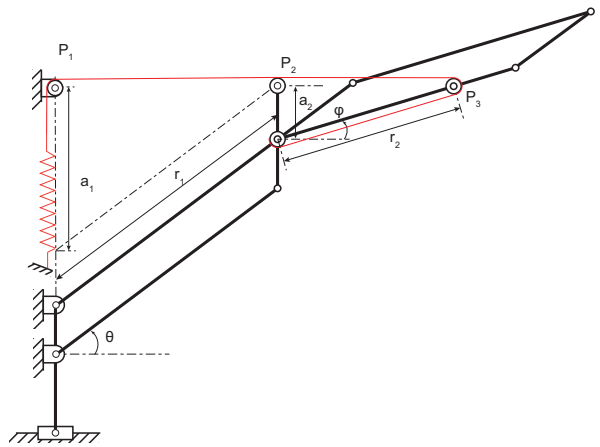


Fig. 6: Definition of the angles

be arranged such that we get the parameters for an equal spring constant.

$$k = \frac{(r_{1g}m_1 + l_4m_2)g}{r_1a_1} = \frac{m_2gr_2g}{r_2a_2} \quad (23)$$

#### 2.4.3 Transition Position

The equations above treats the behaviour of the mechanism as having two independent configurations. It has to be shown that during the transition of the one configuration to the next the potential energy remains the same and does not 'jump' from one configuration to the other. To check this, the angles of the transition position are filled into the potential energy equations for each of the configurations

$$\mathcal{V}(0, -\pi/2)_1 = -m_2r_2g + ka_2r_2 + \frac{1}{2}k(a_1^2 + r_1^2 + a_2^2 + r_2^2) \quad (24)$$

$$\mathcal{V}(0, -\pi/2)_2 = -m_2r_2g + ka_2r_2 + \frac{1}{2}k(a_1^2 + r_1^2 + a_2^2 + r_2^2) \quad (25)$$

The equations show that the potential energy is the same for both configurations in the transition position. Since both the parameters of the mechanism and the spring are chosen according to equations 21 & 22, the mechanism has a constant potential energy through both configurations.

#### 2.4.4 Actual Model

The equations above are formulated using a simplified model of two concentrated masses, the masses for the links and actual masses for the patient's leg still need to be incorporated.

The values for the masses of the links and patient leg were taken from Tseng et al. [2]. In Fig. 7 all the masses and position vectors of the mechanism can be seen. For clarity, the equations are split into the masses of the mechanism and the masses of the patient's leg. All the masses and position

vectors of the mechanism can be seen, are shown to arrive at the following summation:

$$\begin{aligned} \mathcal{V}_g = & (p_1m_3 - p_{10}m_6 - p_{15}m_8 + p_{17}m_9)g \\ & + (p_1 + p_4) \left( \sum_{i=4}^8 m_i \right) g - \\ & \left( \sum_{i=10}^{12} p_i \right) (m_7 + m_8) g + \sin(\theta) \\ & \left( (p_6 + p_7) \left( \sum_{i=4}^8 m_i \right) + (p_{13} + p_{14}) m_8 \right. \\ & \left. + p_2m_2 + p_3m_3 + p_8m_4 + p_{13}m_7 \right) g + \end{aligned} \quad (26)$$

$$\begin{aligned} & \sin(\phi) \left( p_{10}(m_6 + m_2/2) \left( \sum_{i=10}^{12} p_i \right) m_7 + \right. \\ & \left. \left( \left( \sum_{i=10}^{12} p_i \right) + p_{15} \right) m_8 \right) g \end{aligned}$$

$$\begin{aligned} \mathcal{V}_{gl} = & (p_1 + p_4) (m_f + m_c + m_t) g - p_c m_c g - \\ & \left( \left( \sum_{i=10}^{12} p_i \right) + p_{15} + p_f \right) m_f g + \sin(\theta) \\ & \left( (p_6 + p_t) m_t + \left( \left( \sum_{i=6}^8 p_i \right) + p_{18} \right) m_c + \right. \\ & \left. (p_6 + p_7 + p_{13} + p_{14}) m_f \right) g \\ & + \sin(\phi) \left( p_c m_c + \left( \left( \sum_{i=10}^{12} p_i \right) + p_{15} \right. \right. \\ & \left. \left. + p_f \right) m_f \right) g \end{aligned} \quad (27)$$

Because the angle  $\phi_2$  is dependent on angle  $\phi$ , the mass of link two is divided onto the slider joint and onto

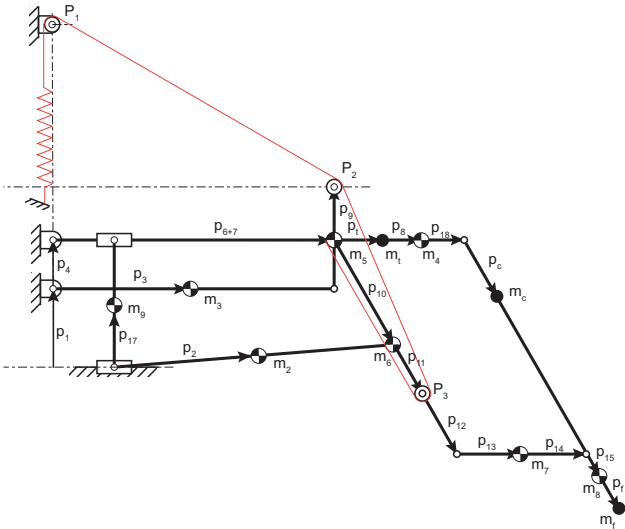


Fig. 7: Mechanism with all masses and position vectors

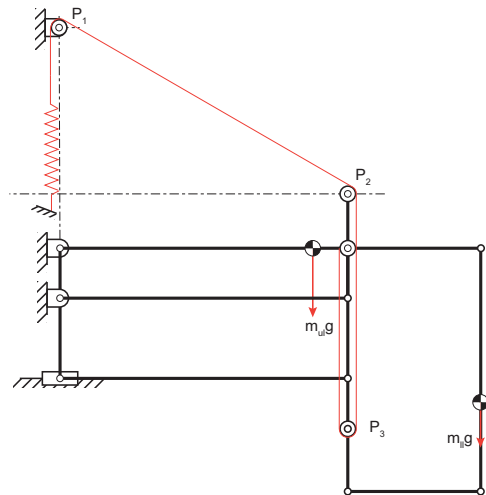


Fig. 8: Mechanism in transition position

link 6. As formulated in equations 18 and 19, the potential energies contained in the spring for the two operation modes are:

$$\mathcal{V}_{s1} = \frac{1}{2}k(r_1^2 + a_1^2 - 2r_1a_1 \sin(\theta)) + \frac{1}{2}k(r_2 + a_2)^2 \quad (28)$$

$$\mathcal{V}_{s2} = \frac{1}{2}k(r_2^2 + a_2^2 - 2r_2a_2 \sin(\phi)) + \frac{1}{2}k(r_1^2 + a_1^2) \quad (29)$$

The variable gravitational potential energies are summed to give the total gravitational potential energies for each angle:

$$\begin{aligned} \mathcal{V}_{g\theta} = & \left( (p_6 + p_7) \left( \sum_{i=4}^8 m_i \right) + (p_{13} + p_{14}) m_8 \right. \\ & \left. + p_2 m_2 + p_3 m_3 + p_8 m_4 + p_{13} m_7 \right) g + \\ & \left( (p_6 + p_t) m_t + \left( \left( \sum_{i=6}^8 p_i \right) + p_{18} \right) m_c \right. \\ & \left. + (p_6 + p_7 + p_{13} + p_{14}) m_f \right) g \end{aligned} \quad (30)$$

$$\begin{aligned} \mathcal{V}_{g\phi} = & \left( p_{10}(m_6 + m_2/2) + \left( \sum_{i=10}^{12} p_i \right) m_7 + \left( \left( \sum_{i=10}^{12} p_i \right) + \right. \right. \\ & \left. \left. p_{15} \right) m_8 \right) g + \\ & \left( p_c m_c + \left( \left( \sum_{i=10}^{12} p_i \right) + p_{15} + p_f \right) m_f \right) g \end{aligned} \quad (31)$$

The parameters in these equations are also taken from Tseng et al. [2]

mass	[kg]
$m_2$	0.13
$m_3$	0.13
$m_4$	1.87
$m_5$	0.13
$m_6$	0.13
$m_7$	0.3
$m_8$	1.17
$m_9$	0.37
$m_t$	8.4
$m_c$	4.4
$m_f$	1.1

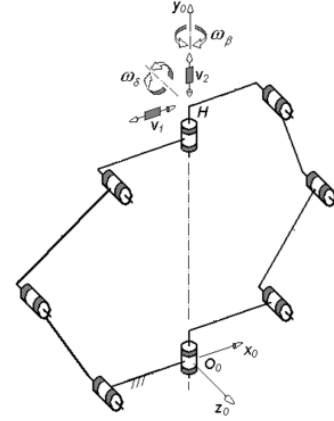
TABLE 1: Masses of the links and body

link	[m]	link	[m]
$p_1$	0	$p_{11}$	0.035
$p_2$	0.075	$p_{12}$	0.04
$p_3$	0.075	$p_{13}$	0.125
$p_4$	0.075	$p_{14}$	0.125
$p_5$	0.07	$p_{15}$	0.056
$p_6$	0.116	$p_{17}$	0.00707
$p_7$	0.035	$p_{18}$	0.187
$p_8$	0.063	$p_t$	0.06
$p_9$	0.075	$p_c$	0.13
$p_{10}$	0.075	$p_f$	0.16

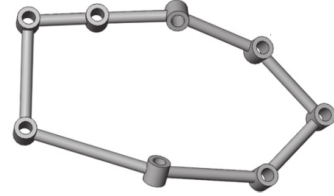
TABLE 2: Length of the vectors on the mechanism

## 2.5 Single Loop, Multiple Dof Mechanisms

The other group of mechanisms that have a generalised static balancing strategy is the single-loop, multiple DoF mechanisms. Our literature study revealed the mechanisms of this group each have similar structures that generally



(a) Mechanism adapted from Gogu [9]



(b) Mechanism adapted from Kong [8]

Fig. 9: Single loop, multiple DoF mechanisms

consist of a ring of revolute joints in different orientations. These different orientations allow the mechanism to rotate in plane for the first configuration and out of plane for the second configuration. The mechanisms exist in different forms and lead to different mobilities. This paper illustrates examples by Kong [8], seen in Fig. 9b and Gogu [9], seen in Fig. 9a because they both have more than one degrees of freedom in all configurations.

In the following, we first discuss the mechanism by Gogu [9], this mechanism is easier to balance because of the alignment of the axes, there are two sets of parallel revolute joints. This means that the joints will always operate in the same plane. To statically balance the mechanism, each link is balanced with respect to the previous link. This is done in two steps: First a horizontal base has to be made using a parallelogram. Second, the next link is balanced from this horizontal base. Gogu [9] shows a device in Fig. 9a that performs these two steps. This mechanism has two operation modes, a 3 DoF, using 6 revolute joints, or 6R mode, and a two DoF, 8R mode. This mechanism is easier to balance because the gravitational potential energy does not change when moving from the 6R to the 8R mode. This means that if the first mode is balanced, the second mode does not require any additional balancing.

The other mechanism shown in Fig. 9b works in a similar fashion only the two out of plane axes are not aligned but have an angle with respect to each other. This makes the balancing slightly more complicated but can be overcome.

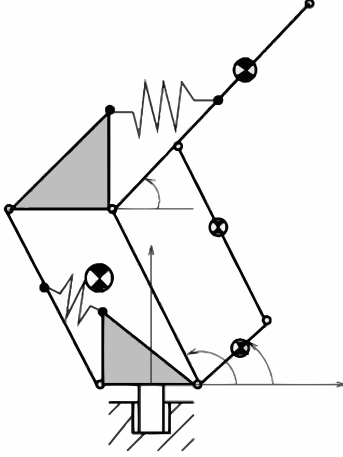


Fig. 10: Balancing mechanism by Gosselin

## 2.6 Proof of SLMD balancing

As noted in the previous section, the SLMD's can be balanced by calculating the balancing conditions from each link with respect to the following link. Both the mechanisms considered for this paper have one configuration with 3 DoF and one with 2 DoF. The balancing mechanism devised by Gosselin, is balanced by four springs so a potential energy balance is required for each spring. This is achieved by balancing each link with respect to the previous link, as described above. In the 3 DoF mode, the location of link 5 at the top also effects the balancing. This mechanism is essentially a parallel mechanism, the proof of concept for which has also been provided by Gosselin [10]

The x component of the centre of mass: The potential energies of the weight on each link is described.

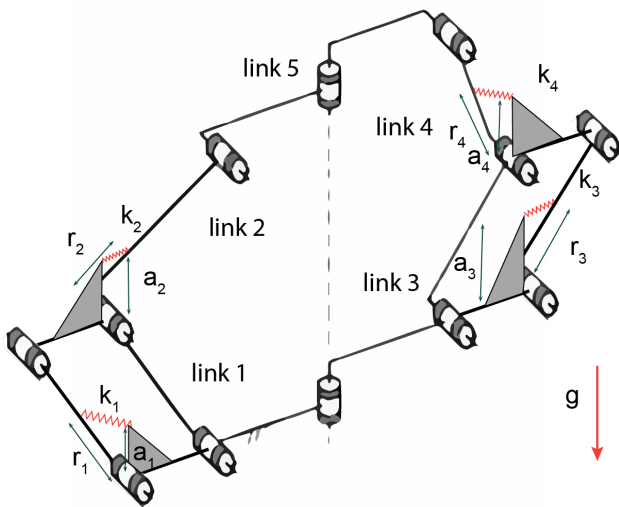


Fig. 11: Balanced mechanism by Gogu [9]

$$V_{g4} = (m_5/2l_4 + m_4l_4/2)\sin(\phi_4) \quad (32)$$

$$V_{g3} = (l_3(m_4 + m_5/2) + m_3l_3/2)\sin(\phi_3) \quad (33)$$

$$V_{g2} = (m_5/2l_2 + m_2l_2/2)\sin(\phi_2) \quad (34)$$

$$V_{g1} = (l_1(m_2 + m_5/2) + m_1l_1/2)\sin(\phi_1) \quad (35)$$

Next the potential energy of the springs are listed, first by defining the spring lengths.

$$l_{si} = \sqrt{a_i^2 + r_i^2 - 2a_i r_i \sin(\phi_i)} \quad (36)$$

Where  $i$  is the link number 1 to 4.

The equation for the spring length is added to the formula for the potential energy:

$$V_{tot} = mgr_g \sin(\phi) + 1/2k(a^2 + r^2) - kar \sin(\phi) \quad (37)$$

So the balancing condition for each spring becomes:

$$C_4 = (m_5/2l_4 + m_4l_4/2) - k_4a_4r_4 \quad (38)$$

$$C_3 = (l_3(m_4 + m_5/2) + m_3l_3/2) - k_3a_3r_3 \quad (39)$$

$$C_2 = (m_5/2l_2 + m_2l_2/2) - k_2a_2r_2 \quad (40)$$

$$C_1 = (l_1(m_2 + m_5/2) + m_1l_1/2) - k_1a_1r_1 \quad (41)$$

$$(42)$$

With  $C$  being the balancing condition for each spring.

Kongs [8] mechanism as shown in Fig. 12 is balanced in exactly the same way except for the fact that the out of plane joints are not parallel but are at an angle. Because this angle is constant for the whole mechanism, gravity also works at a different angle. However, because this is the same for each mass, it is a constant that can be implemented in the spring constant.

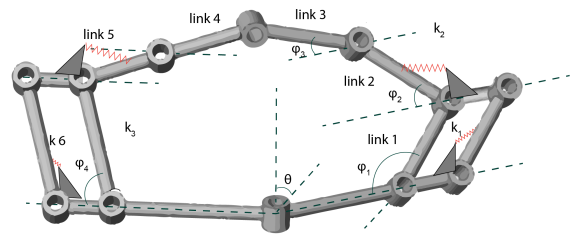


Fig. 12: Balanced mechanism by Kong [8]

## 3 RESULTS

### 3.1 Simulation Results

To validate this proof, the first step was to make a simulation in the multibody dynamics software *MSC ADAMS*. This

software is used because all of the components can be realistically simulated including a cable connected the spring.

First, the required spring constant is calculated for each mode; this constant is independent in each mode but has to be equal so that the mechanism can be balanced with one spring. To achieve the same spring constant, the connection points need to be shifted iteratively.

The model in ADAMS is constructed using 'Link' parts as shown in the the rendering of the mechanism in Fig. ???. In an actual model this mechanism could be built using mostly revolute joints as connections between the links. In the simulation however, this would over-constrain the mechanism. To prevent this the mechanism is constructed using multiple joints with varying degrees of freedom. ADAMS provides an additional toolbox which enables the cable and pulleys to be generated.

The total cable length can be split into constant lengths, which do not change length when the mechanism is in motion and variable cable lengths which do change. The pulley diameters must all be equal in order for the cable length of the constant cable lengths to remain constant while in motion. As described above, the desired behaviour of a statically balanced mechanism is that the mechanism remains in the same place when left in a certain position. First, the required spring constant is calculated for each mode; this constant is independent in each mode but has to be equal so that the mechanism can be balanced with one spring. To achieve the same spring constant, the connection points need to be shifted iteratively. To verify if the energy does remain constant, two motions are installed on the mechanism that move the mechanism through the same movements that a patient would perform. In the plot in figure 14 the potential energy of the mechanism during this motion is shown.

The plot reveals two lines, the gravitational potential energy and the total potential energy of the mechanism

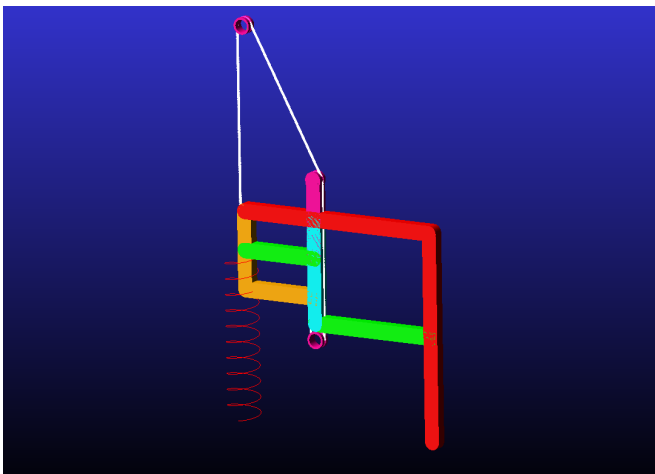


Fig. 13: Render of the simulation

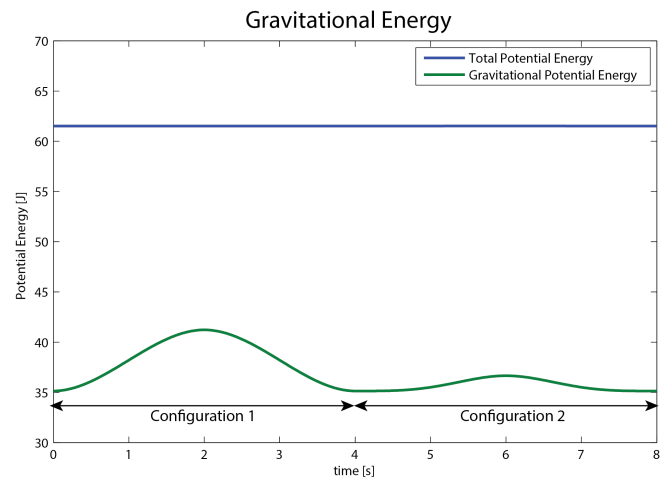


Fig. 14: Plot of the potential energy of the mechanism

including the spring. In the green graph, two peaks can be identified, these correspond to the two motions that the mechanism makes. The first peak is the extension of the upper leg, or first configuration, the second peak is the extension of the lower leg or second configuration. When the potential energy of the spring is added to this, the blue line shows that the potential energy remains constant. This confirms the behaviour calculated in the previous section and means that the mechanism is statically balanced.

### 3.2 Physical Model

The second verification step is carried out by means of an experiment using a physical model. For this, a set-up is made using a scale model of the mechanism by Tseng. The spring balancing of the mechanism is designed in accordance with the theory for single spring balancing as previously explained. The goal of the experiment is to measure the behaviour associated with a statically balanced mechanism. The dimensions of the mechanism and the spring stiffness were derived using the formulas above; these are chosen such that the potential energy of the mechanism remains constant. Ideally, the potential energy of the mechanism would therefore be measured, which is not possible. The derivative of the potential energy for this mechanism is the moment for each of the configuration, which can be possible to measured. Because the design is such that the potential energy remains constant, the moment of the two motions should remain zero for the entire range of motion of the mechanism.

Figure 15 shows the mechanism used for testing. The moment is measured through two cables, one for each configuration. Each cable is wound around one of the discs seen on the left and right side of the top link. This cable leads to a Zwick Universal Testing Machine that moves at a constant velocity and registers the force at each location. Additional weights are attached to the mechanism during the testing of each mode. Because the mechanisms is calculated to be statically balanced and there is some friction in the mechanism, the weight ensures that the mechanism will lower again after raising each

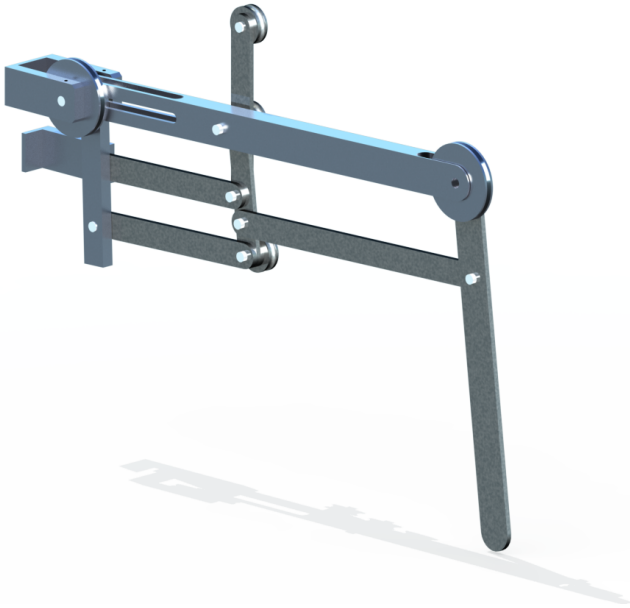


Fig. 15: Render of the mechanism in Solidworks without spring

configuration. Because the additional weight is attached to a link in each configuration, the effect is measured as a sinusoidal extra moment through the pulley. The universal testing machine performs an up and down motion from which a hysteresis loop is obtained. The mechanism is proved to be statically balanced if, after subtraction of the extra masses, the average of the hysteresis loop is a horizontal line of around zero.

In Fig. 17 the hysteresis loop can be seen, it shows the measured forces for each configuration. The blue line represents an average of five repetitions of the mechanism

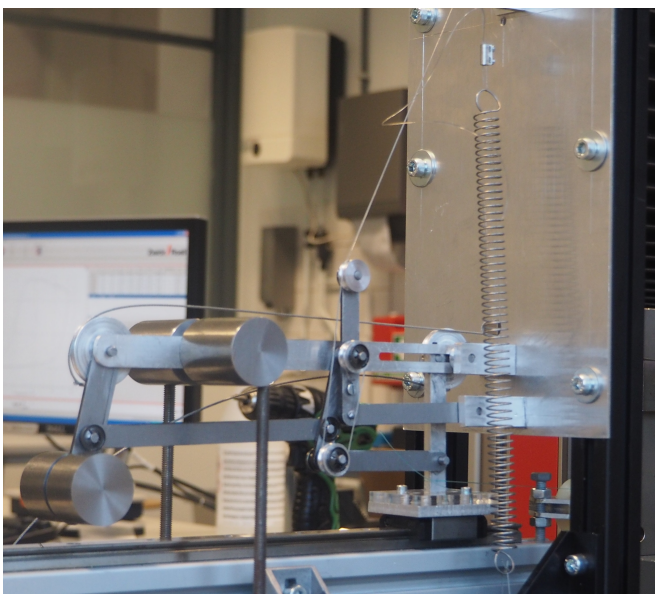


Fig. 16: Experimental Set-up

in an up and down motion. The masses are directly connected to the links, because the angle of the mechanism is known, the influence of these masses are subtracted from the measure force. The red line is the force after compensation. The black line is the average of the shared path of the red lines. For both configurations it can be seen that it is a horizontal line of around zero Newton. This means it can be assumed that both of the configurations are statically balanced by the same spring.

## 4 DISCUSSION

### 4.1 Tseng mechanism balancing

Despite the fact that both forms of validation are generally successful, there are some aspects that are not perfect. The potential energy plot, obtained from the ADAMS simulation does not show an exactly flat curve. Instead there seems to be a peak of about  $0.009J$  in the potential energy during the lower leg mode. This appears to be due to a small error somewhere in the simulation which a lengthy search could not resolve. The error is expected to come from the dimensions of the cable that is used. After iteratively changing the position of the pulleys of the first configuration it was possible to obtain a flat potential energy plot. Importantly, the simulation did reveal, however, that the potential energy does not 'jump' when moving from the first to the second configuration. This is why it is assumed that the peak in the plot is due to an error instead of the model being flawed.

The second validation step was the physical model. The preferred outcome was that the physical model would resolve any doubts left by the simulation. However, while the physical model does indeed show that the mechanism is mostly perfectly balanced, due to friction, the graph shows additional distortion. Moreover, there is a certain amount of flexibility in the mechanism. This means that it is not possible to take the whole path of the mechanism to show that the average was zero.

## 5 CONCLUSION

This paper introduces generalised static balancing methods for single loop reconfigurable mechanisms. The general static balancing strategy of two different groups of reconfigurable mechanisms is shown i.e., single-loop, single DoF and single-loop, multiple DoF. The strategy for each of the groups is mathematically elaborated and a sketch of a possible solution provided. Single loop, single DoF mechanisms are more elaborately discussed facilitated by a clear application. The expectation that single loop, single degree of freedom mechanisms can be balanced using a single spring is proven to be valid for two mechanisms. It is now known that two separate configurations can be balanced using a single spring.

A simulation and a physical experiment were conducted for the rehabilitation device by Tseng et al. which confirms the expected behaviour. The solution presented for the

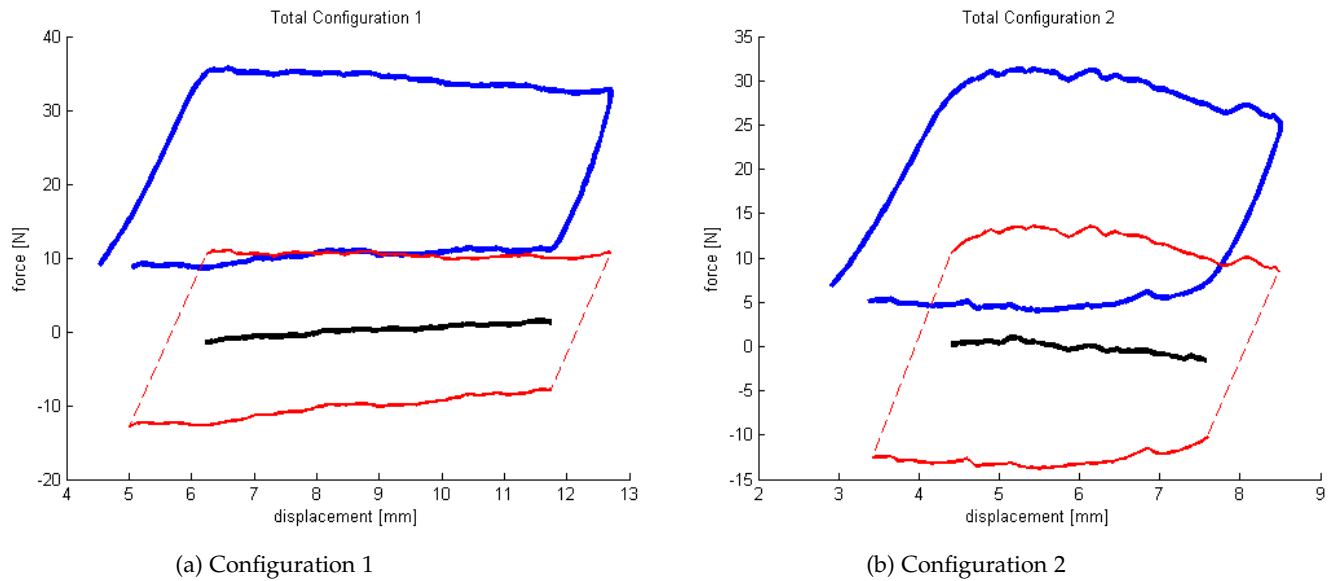


Fig. 17: Hysteresis loops of both configurations

mechanism by Tseng et al. leads to a simplification of the mechanism because it is shown that one spring can be used to balance both configurations instead of two. Also is shown that a cable- and pulley-based solution is a valid alternative to expensive zero free-length springs. These theories can lead to a more efficient balancing of reconfigurable mechanisms and provide guidance for anyone looking to balance single loop reconfigurable mechanisms.

## 6 REFERENCES

### REFERENCES

- [1] P. D. Robertson, C.-H. Kuo, and J. L. Herder, "A Compatibility Study Of Static Balancing In Reconfigurable Mechanisms," in *Proc. ASME Int. Des. Eng. Tech. Conf. Comput. Inf. Eng. Conf.*, (Charlotte, NC), 2016.
- [2] T.-Y. Tseng, W.-C. Hsu, L.-F. Lin, and C.-H. Kuo, "Design and Experimental Evaluation of a Reconfigurable Gravity-Free Muscle Training Assistive Device for Lower-Limb Paralysis Patients," in *Proc. ASME 2015 Int. Des. Eng. Tech. Conf. Comput. Inf. Eng. Conf.*, (Boston, Massachusetts), ASME, 2015.
- [3] K. Wohlhart, "Kinematotropic Linkages," in *Recent Adv. Robot Kinemat.*, ch. 7, pp. 359–368, Springer Netherlands, 1996.
- [4] R. Fisher, R. P. Podhorodeski, and S. B. Nogleby, "Design of a reconfigurable planar parallel manipulator," *J. Robot. Syst.*, vol. 21, no. 12, pp. 665–675, 2004.
- [5] D. Z. Gao, G. W. Cai, H. Shi, and Y. C. Pan, "Adjacency Matrix Based Analysis on a Novel Metamorphic Manual Operation Sugarcane Loader," *Appl. Mech. Mater.*, vol. 397-400, pp. 1529–1533, 2013.
- [6] J. L. Herder, *Energy-free systems: theory, conception, and design of statically balanced spring mechanisms*. PhD thesis, Delft University of Technology, 2001.
- [7] A. Muller, "On the Concept of Mobility Used in Robotics," in *Proc. IDETC/CIE*, (San Diego, CA), pp. 1275–1284, ASME, 2009.
- [8] X. Kong and C. Huang, "Type synthesis of single-DOF single-loop mechanisms with two operation modes," in *2009 ASME/IFToMM Int. Conf. Reconfigurable Mech. Robot.*, (London, UK), pp. 136–141, ASME/IFToMM, 2009.
- [9] G. Gogu, "Branching singularities in kinematotropic parallel mechanisms," 2009.

- [10] C. M. Gosselin and J. Wang, "On the design of gravity-compensated six-degree-of-freedom parallel mechanisms," *Proceedings. 1998 IEEE Int. Conf. Robot. Autom.*, vol. 3, no. May, pp. 2287–2294, 1998.



2

Review Paper

Proceedings of the ASME 2016 International Design Engineering Technical Conferences &  
Mechanisms and Robotics Conference  
IDETC/CIE 2016  
August 21-24, 2016, Charlotte, USA

**IDETC2016-59281**

## A COMPATIBILITY STUDY OF STATIC BALANCING IN RECONFIGURABLE MECHANISMS

**P.D. Robertson**

Faculty of Materials, Mechanical  
and Maritime Engineering  
Department of BioMechanical Engineering  
Delft University of Technology  
Delft, The Netherlands  
Email: p.d.robertson@student.tudelft.nl

**C.-H. Kuo**

Department of Mechanical Engineering  
National Taiwan University of  
Science and Technology  
Taipei, Taiwan  
Email: chkuo717@mail.ntust.edu.tw

**J.L. Herder\***

Faculty of Materials, Mechanical  
and Maritime Engineering  
Department of Precision and  
Microsystems Engineering  
Delft University of Technology  
Delft, The Netherlands  
Email: j.l.herder@tudelft.nl

### ABSTRACT

*Reconfigurable mechanisms are a group of mechanisms that can change their topology or mobility while in operation. This property can add flexibility of the use of the mechanisms in constrained environments. Some situations require these mechanisms to be statically balanced. One example is a statically balanced lower-limb rehabilitation device, allowing patients who suffer from lower-limb paralysis to exercise without the need for a therapist to guide them. This mechanism by Tseng et al. [1] is one of the very few examples of a statically balanced reconfigurable mechanism. From literature it is known that there is no general way to statically balance these mechanisms. This paper aims to create an overview of the methods that can be applied by making a classification of reconfigurable mechanisms based on the intrinsic properties, then reviewing each group of this overview to find a generalised static balancing method. Only two mechanism groups show high compatibility with static balancing. One of these groups could be balanced using a single spring. The other shows the property that if one operation mode is balanced, no additional springs are needed for the other mode. Applying these techniques could reduce the overall complexity of the mechanism.*

### INTRODUCTION

Mechanisms and linkages are typically designed to perform a single motion or task that will not change over time [2]. Reconfigurable mechanisms, a class of mechanisms with the ability to change topology or mobility during operation, represent an alternative to conventional mechanisms. This property can significantly enhance flexibility of mechanisms in constrained environments such as manufacturing, medical devices and robotics [3]. Reconfigurable mechanisms first garnered attention with the development of new families of mechanisms such as Kinematotropic mechanisms presented by Wohlhart in 1996 [4] and Metamorphic mechanisms in 1999 by Dai and Rees Jones [5]. Since then, multiple authors contributed to this field in the form of analysis, categorisation and synthesis of these types of mechanisms.

One example of a reconfigurable mechanism is defined by Tseng et al. [1] who designed a mechanism for rehabilitation purposes for patients suffering from lower limb paralysis. The patients are able to activate their muscles but are not strong enough to lift their leg against gravity. Traditionally, rehabilitation exercises were very labour intensive for the therapist who has to manually lift and support the leg during the training. The reconfigurability allows the mechanism to support two leg motions of the patient. To replace the physical effort of

\*Address all correspondence to this author.

therapists, the proposed device uses a reconfigurable mechanism to assist two leg motions of the patient and two springs to counterbalance the static load. With the leg balanced, the patient is able to perform the exercise without the use of additional manual support. This was the first mechanism to combine the fields of reconfigurable mechanisms and static balancing.

A system is statically balanced if the potential energy within that system remains constant throughout its range of motion. There are numerous ways to achieve this, the oldest being a counterweight to negate the gravitational force of an object [6]. As mentioned above, another way is to use springs to balance the gravitational force of an object. This form of static balancing shall be considered for the purpose of this research.

Though both the fields of reconfigurable mechanisms and static balancing are well published, there are no known contributions on the combination of these subjects. Therefore there are no general methods known on how to balance specific types of reconfigurable mechanisms. We can expect however that by analysing the special properties of these mechanisms some interesting static balancing behaviour can be found. This study aims to show how these two fields are compatible.

From literature an overview of existing reconfigurable mechanisms is created based on the mechanism characteristics. Then a generalised static balancing strategy is looked for by checking each group for its compatibility with static balancing.

## METHODS

### Search Methods

Prior to researching the categorisation of multiple reconfigurable mechanisms, an extensive literature search was undertaken to determine whether there was no other mention of statically balanced reconfigurable mechanisms. Scopus and Google Scholar were the main source of references. Reconfigurable mechanism was searched for as well as closely related synonyms:

Reconfigurable mechanism  
 Mechanism with Variable Topology  
 Mechanism with multiple operation mode  
 Kinematotropic  
 Metamorphic

These search words were combined with general terms from static balancing:

Static Balancing  
 Gravity Balancing

This combination of search words did not lead to literature that covered both static balancing and reconfigurable mecha-

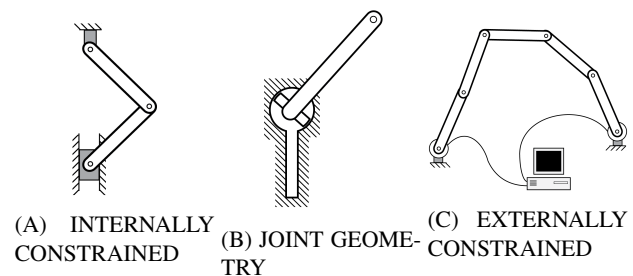


FIGURE 1: RECONFIGURATION METHODS

nisms.

Next a literature research was conducted that lead to categorisation of the field of reconfigurable mechanisms. The search term 'reconfigurable' has many different applications. In order to arrive at relevant results, only mechanisms that were reconfigurable while the mechanism was in operation were selected. The mechanisms found were placed in an overview with categories based on reconfigurability method and mechanism structure.

## Reconfigurable Mechanisms

**Configuration and Topology** A reconfigurable mechanism is a mechanism that can change its configuration during operation [3]. There is a difference in reconfigurable mechanisms and mechanisms with variable topology. In kinematics, topology is an intrinsic property of a mechanism or linkage that, according to Kuo [2], describes the types, numbers, adjacency and incidence of links and joints of a mechanism. The topology of a mechanism is an invariant description of the mechanism structure. Topological configuration [2] is derived from the topology of a mechanism and also takes the relative orientation of links and joints into account.

**Reconfiguration Methods** Mechanisms can be classified by their working principles. Slaboch and Voglewede [3] showed that there are three ways to reconfigure a mechanism:

1. Due to an intrinsic constraint.
2. Due to joint geometry
3. Due to external constraints

In Fig. 1 we can see these reconfiguration methods in a simplified example. Intrinsically constrained mechanisms reconfigure themselves using joint constraints, internal forces etc., as shown in Fig. 1A which depicts a double pendulum constrained to be a slider-crank mechanism. Figure 1B shows an example of a mechanism based on joint geometry, the link has to rotate as a revolute joint to a certain position so that it can translate through the prismatic joint. Externally constrained

mechanisms can be configured using elements such as lockable joints and actuators, shown in Fig. 1C.

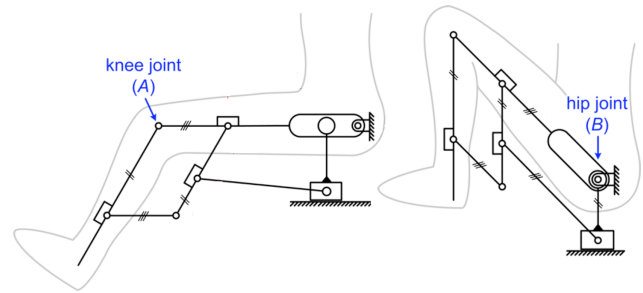
The methods mentioned above can be used to reconfigure mechanisms. The following section describes the numerous ways in which a mechanism can be reconfigured. According to Kuo et al., 2009 [2], there are four different properties that can be changed that result in a different topology or topological configuration.

1. The effective number of links and joints
2. The kinematic types of certain joints
3. The adjacency and incidence of links and joints
4. The relative arrangement between joints

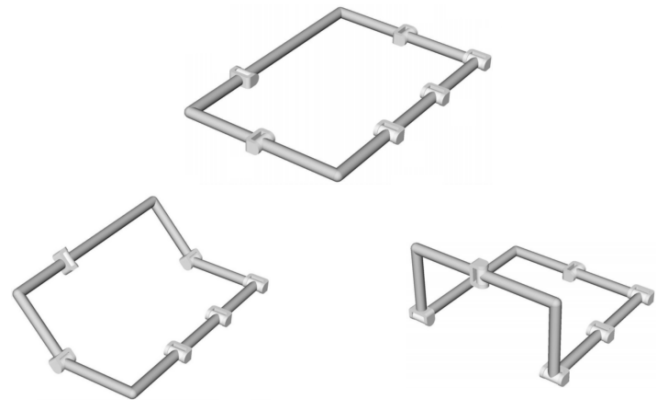
If a mechanism complies with one or more of these statements it can be classified as a reconfigurable mechanism. The first three statements influence the topology of a mechanism, if therefore a mechanism complies with one of these criteria it also qualifies as a mechanism with variable topology (MVT). If a mechanism complies with only the last statement, the topology of the mechanism doesn't change during the operation and the mechanism is classified only as a reconfigurable mechanism.

### Categorisation

An overview of mechanisms is created to identify static balancing strategies in groups of reconfigurable mechanisms. The following hierarchy is used for the structure of the table. The first division is between single and multi-loop mechanisms as this, to a very large extent, determines the mechanism behaviour. The second division is based on the type of reconfiguration strategy. Lastly the maximum mobility in the operation modes is used as a measure for the behaviour. These categories generate a table with twelve different groups. A wide selection of mechanisms is placed in the overview in table 1a. The purpose of the table is to find generalised balancing strategies for each group. As can be seen from the overview, not all categories are equally developed. This table does not mean to identify all the mechanisms and their variations found in literature, rather to provide a representative overview of mechanisms found. Alongside the divisions in mechanisms described above, there are two specific types of reconfigurable mechanisms named in literature, Kinematotropic mechanisms and Metamorphic mechanisms. Wohlhart conceived the term Kinematotropic mechanisms in 1996 for "mechanisms that change their topology based on the input parameters" [4]. Metamorphic mechanisms are mechanisms categorised by Dai and Rees Jones [5] in 1999 that change their number of effective links when moving through different configurations or that have a singular geometrical condition that makes it behave differently. Much of the literature is concentrated around these two mechanism groups. When a mechanism is of one of these types it is also mentioned in the overview.



(A) MECHANISM BY TSENG ET AL. [1]



(B) MECHANISM BY MÜLLER [15]

**FIGURE 2:** MECHANISMS WITH DIFFERENT MOTION ORIENTATION

**Intrinsic constraints** The largest group in the table is the group that works using internal constraints. In this group there are significant differences between the single and multiple loop mechanisms as well as between the single and multiple degree of freedom.

The single loop, single DOF mechanisms have a mobility of one in each of the operation modes [14]. Most of the mechanisms in this group are found to have two configurations. There are some that make an exception based on their structure, this is addressed below. Though the mobility of these mechanisms is the same, the direction orientation of the configurations relative to each other is different. An example of this difference is shown in the two mechanisms below. In Fig. 2A we can see that the two operation modes operate in the same plane as the mechanism whereas with the mechanism in Fig. 2B the operation modes are out of the mechanism plane. Another difference within this group is the type of motion, the mechanism in Fig. 2A switches from a 3RP to a 4R mechanism while the mechanism in Fig. 2B remains a 2R mechanism in both modes.

**TABLE 1: TYPOLOGY VERSUS CONFIGURATION TYPE**

	Single Loop		Multiple Loop	
	Single DOF	Multiple DOF	Single DOF	Multiple DOF
Intrinsic Constraint	Tseng [1] 2 modes 1 DOF Kinematotropic	Gogu [7] 2 modes 2-3 DOF Kinematotropic	Yan [8] 3 modes 1-0-1 DOF Metamorphic	Gao [9] 3 modes 1-3-4 DOF Metamorphic
	Gogu [7] 2 modes 1 DOF Kinematotropic	Kong [10] 2 modes 2-3 DOF Kinematotropic	Gogu [7] 2 modes 1 DOF Kinematotropic	Galletti [11] 2 modes 1-3 DOF Kinematotropic
	Kong [12] 2 modes 1 DOF Kinematotropic	Galletti [11] 3 modes 2-3 DOF Kinematotropic	Hao [13] 2 modes 1 DOF Kinematotropic	Gogu [7] 2 modes 1-2 DOF Kinematotropic
	Galletti [11] 2 modes 1 DOF Kinematotropic			Kong [14] 3 modes 3 DOF Kinematotropic
	Müller [15] 2 modes 1 DOF Kinematotropic			
	Song [16] 3 modes 1 DOF			
External Constraint	Balli [17] 1 DOF 3 modes	Ye [18] multiple examples Metamorphic		Fisher [19] 3 DOF Metamorphic
				Palpacelli [20] 3 DOF Metamorphic
Joint Geometry	Zhang [21] 3 modes 1 DOF			Gan [22] 8 modes Metamorphic

(a) Table with an overview of the mechanisms found subdivided by topology of the mechanism versus the reconfiguration method described above. Each cell contains the name and reference of the author, number of operation mode, number of degrees of freedom in each mode and type of reconfigurable mechanism.

In the single loop, multiple DOF mechanism group two working principles can be identified. The first is shown in Fig. 3 by Gogu [7] which has an 8R ring of revolute joints, where two R-joints are rotated ninety degrees with respect to the others. This allows the mechanism to enter the second operation mode by rotating out of plane. The mechanism changes from 3 DOF in the 6R mode to 2 DOF in the 8R mode. A comparable

working principle can be found in the mechanism by Kong et al. [12] although the R-joints are rotated by 45 degrees instead of 90.

The other working principle relies on multiple pairs of joints that move in and out of alignment, enabling parts of the mechanism to become mobile or be locked.

The example found of this mechanism is shown by Galletti and Fanghella [11] in Fig. 4. Though this mechanism is different

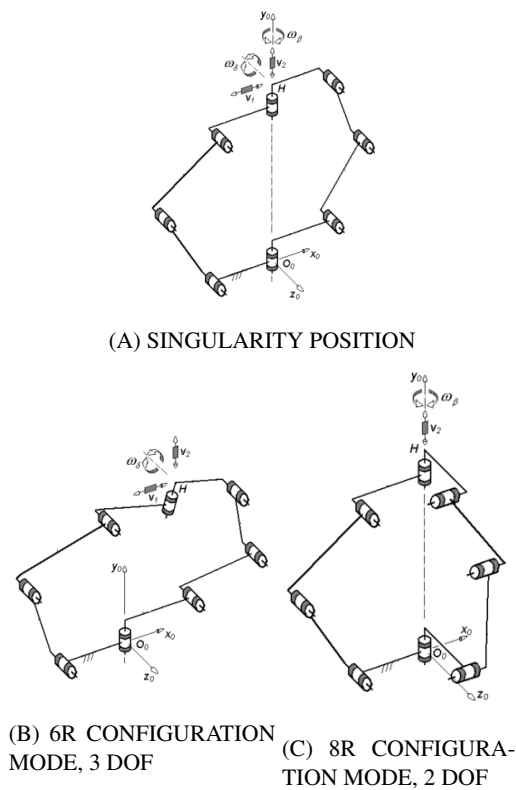


FIGURE 3: MECHANISM BY GOGU [7]

because of the fact that some of the modes turn this mechanism into a multiple loop mechanism. This mechanism therefore spans multiple groups.

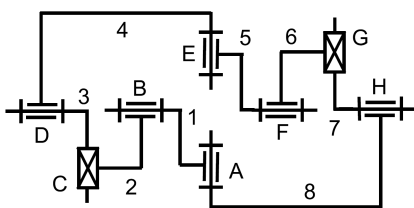
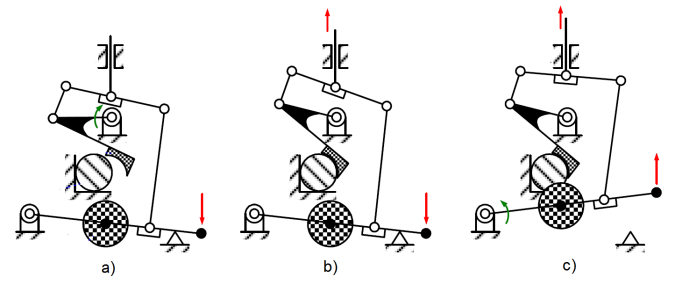
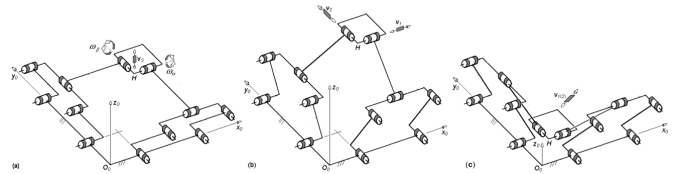


FIGURE 4: SINGLE LOOP MECHANISM BY GALLETTI AND FANGHELLA [11]

The remaining two groups in the intrinsically constrained category show a lot more variation within the categories. With additional mechanism loops a greater number of possibilities for reconfiguration can be formed. Two examples in the single DOF category are shown in Fig. 5. In this example we can clearly see large differences within this group. The first image



(A) METAMORPHIC 7 BAR MECHANISM BY YAN AND KUO [8]



(B) KINEMATOTROPIC PARALLEL MECHANISM BY GOGU [7]

FIGURE 5: TWO MULTIPLE LOOP SINGLE DOF MECHANISMS

5A gives a schematic of a metamorphic steel clamping and sawing device [8] which is reconfigurable because of the effective number of links that changes when the steel beam is being clamped and/or sawn. The second mechanism in Fig. 5B is a kinematotropic mechanism that changes the relative arrangements of the joints; the platform can move up or down from the singularity position.

This variability also holds for the multiple loop multiple DOF mechanisms where the increased number of loops leads to a wider set of mechanisms.

**External Constraints** The mechanisms in this group change topology or configuration because of externally enforced constraints such as actuators or lockable joints which influence the behaviour of the mechanism. This technique is for instance applied in robotics in order for the robot to be able to perform different motions using the same mechanism. Although this is a widely applied technique, the mechanisms are often not classified as a reconfigurable mechanism. Palpacelli et al. [20] show a parallel mechanism using universal joints which are able to lock in a certain position limiting the mobility of the stage, Fig. 6. The mechanism is able to switch from a purely rotational, Fig. 6A to a purely translational stage, Fig. 6B, by locking certain motions of a universal joint indicated in red.

Because this technique can be widely applied to different types of links and joints, many mechanisms can in this way be made reconfigurable. Thus except for the multiple loop, single

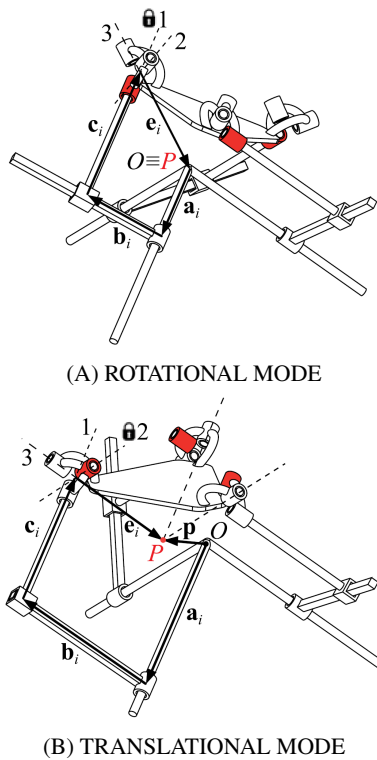


**FIGURE 6:** PARALLEL MECHANISM BY PALPACELLI [20] USING LOCKABLE JOINTS

DOF mechanisms this technique was found for all groups.

**Joint Geometry** There are not many examples of reconfigurable mechanisms of which the working principle relies on joint geometry. One example can be seen in Fig. 7 which is one of the few examples that provides a full mechanism. The mechanism works by spherical joints that only allow motions in certain directions, thus creating a finite amount of modes. Another is a parallel mechanism by Gan et al., 2011 [22] where the geometry in the joint can change to switch the axes of rotation for each of

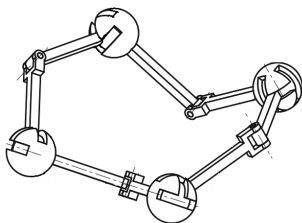


**FIGURE 7:** EXAMPLE OF A MECHANISM RECONFIGURABLE BY JOINT GEOMETRY BY ZHANG, 2009 [23]

the legs of the parallel mechanism. There are more examples of individual joints that could be applied in reconfigurable mechanisms e.g., by Slaboch and Voglewede [3] but these have not been considered for the overview since they have not been used in a full mechanism.

### Static Balancing Methods

There are various different methods that can be used to balance an object like using counterweights or springs. For the purpose of this paper, only gravity balancing using springs to equilibrate the gravitational forces is considered. Additionally the springs that will be considered are 'ideal' or zero free-length springs. This means that the force in the spring is proportional to the length of the spring as opposed to the extension of the spring [24]. Normal springs can overcome this property but for the purpose of this research they will not be considered.

**Single DOF** There are different approaches to statically balance a mass, but the principle remains the same. Herder [24] demonstrates this on the Basic Gravity Equilibrator in Fig. 8. This simple Fig. shows a mass at the end of a link balanced by a spring. For this mechanism to be in equilibrium throughout its range of motion the parameters for the attachment of the spring have to be chosen. The criteria for these parameters can be determined by considering the potential energy of the system.

$$V_{tot} = \frac{1}{2}k(a^2 + r^2) - rka \cos(\phi) + mgr_m \cos(\phi) \quad (1)$$

With  $\phi$  being the angle between the link and the positive vertical and  $k$  the spring constant. Leading to the parameters:

$$mgr_m = rka \quad (2)$$

By choosing the parameters according to equation 2, the potential energy will remain constant throughout the range of motion of the mechanism.

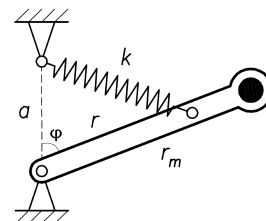


**FIGURE 8:** BASIC GRAVITY EQUILIBRATOR [24]

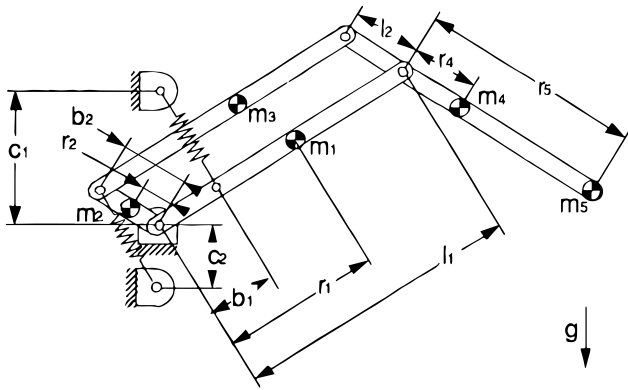


FIGURE 9: TWO DEGREE OF FREEDOM EQUILIBRATOR BY STREIT AND SHIN [25]

**Multiple DOF** For multiple degree of freedom balancing, additional springs and supporting links are needed. According to Streit and Shin [25], in theory any planar rigid body mechanisms can be balanced by application of the two degree of freedom equilibrator. This is proved using an extended two degree of freedom parallelogram mechanism shown in Fig. 9. All the links of the mechanism are balanced using two springs, again by choosing the parameters such that the potential energy in the system remains constant. These parameters are then chosen according to the following equation:

$$[m_1 r_1 + m_3 r_3 + m_4 l_4 + m_5 l_1]g = k_1 b_1 c_1 \quad (3)$$

$$[m_2 r_2 + m_3 l_2 - m_4 r_4 - m_5 r_5] = k_2 b_2 c_2 \quad (4)$$

A link can be attached in its centre of mass to the end of this mechanism so that it is balanced in all three degrees of freedom.

By pivoting replacing the revolute joint, where the parallelogram connects to ground for a spherical joint, the two DOF equilibrator concept can be extended for spatial motions, demonstrated in Fig. 10. By adding the spherical joint the mobility is increased by three by balancing the rotations about the spherical joint.

Gosselin and Wang [26] showed how to balance additional links in a chain by adding parallelograms to create a base that stays in the same orientation when the link rotates. This means the following link is balanced by attaching a spring from the base to that link.

## RESULTS

Each category discussed in the previous section is evaluated to attempt to find a generalisable static balancing strategy.

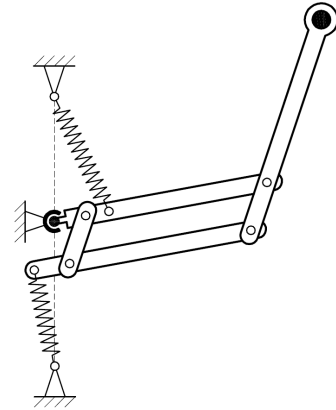


FIGURE 10: SPACIAL BALANCER BY HERDER [24]

**Intrinsic constraint** Each mode of the single loop single DOF mechanisms can be balanced with one spring. Because one mode can be operational at a time, one point could be found from where both modes can be balanced simultaneously. From the mechanism by Herder [24] we know that the attachment point of the spring should be in line with the axis of rotation of the link. The attachment point could be somewhere along the vertical line in Fig. 12. This could be one way to balance the mechanism by Müller [15], shown in Fig. 2B, by attaching the spring above the intersection of the two axes of the joints.

By finding a point on the mechanism from where both modes can be balanced, the single loop single DOF mechanisms may be balanced, but it can be required to shift the attachment point of the spring. This step is required to potentially balance the mechanism by Tseng et al. [1].

For the mechanisms in the single loop multiple DOF category, like in Fig. 3A, a general balancing strategy can be found. By balancing each link in the loop, the mechanism should

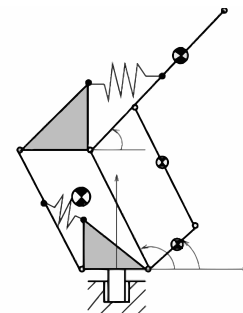


FIGURE 11: BALANCING LINKS IN A CHAIN ADAPTED FROM GOSSELIN [26]

not require additional springs while moving into the other mode. In the previous section, a balancing mechanism by Gosselin [26] was shown that balances links in a chain. This technique can be applied to the single loop, multiple DOF mechanism group to balance the links.

The rest of the mechanisms in this category do not have a generalisable balancing strategy.

**External Constraint** The mechanisms in this group heavily rely on externally determined behaviour. Even though these mechanisms could potentially benefit from static balancing to e.g., reduce static motor torques, no general static balancing technique can be applied because each mechanism behaves in a different fashion.

**Joint Geometry** In this group there are too few mechanisms to be able to generalise the behaviour. These mechanisms can be balanced but due to the many possible variations there is no point to balance them as a group.

## DISCUSSION

The mechanisms in the overview are a representation of all the different reconfigurable mechanisms. Because of the wide variety found in reconfigurable mechanisms or mechanisms with variable topology, a large proportion of them are not classified as such. This makes searching and grouping of the mechanisms limited because without these terms finding more mechanisms is more challenging.

A lot of the literature found on the subject of reconfigurable mechanisms and mechanisms with variable topology are written with the purpose of classification, synthesis or kinematic analysis. This means that personal insights and choices of mechanism orientation and gravitational direction influences the review of

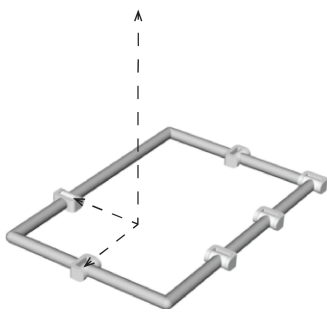


**FIGURE 12:** MECHANISM BY MÜLLER [15] WITH ROTATION LINES

the mechanism for static balancing.

The overview was constructed using the reconfiguration methods formulated by Kuo et al. [2] and divisions based on mechanism structure. This division works well for the simple single loop mechanisms but for the multiple loop mechanisms the variety found seems to be too great to find generalisable behaviour. To solve this, more categories were introduced to create smaller groups. The other division in reconfigurable mechanisms, the reconfiguration strategies, were introduced as another categorisation. This did not solve the problem because many of the mechanisms in the multiple loop groups seemed to rely on multiple strategies, still leaving the group fragmented.

## CONCLUSION

In this paper reconfigurable mechanisms and static balancing were compared and combined in search of general strategies to gravity balance this type of mechanism. The overview presented shows that special properties of certain reconfigurable mechanism categories can lead to specific static balancing strategies.

The field of reconfigurable mechanisms was categorised based on reconfiguration methods and mechanism structure. This led to twelve groups of mechanisms.

It is now known that the behaviour of most of the groups are too varied or inconsistent to be able to indicate a single general balancing strategy.

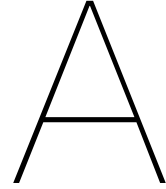
There are two groups of which the mechanisms are similar enough to indicate a single static balancing strategy within those groups. These are the intrinsically constrained single loop single degree of freedom mechanisms and the intrinsically constrained single loop, multiple degree of freedom mechanisms.

The single loop, single degree of freedom mechanisms have the potential to be balanced using a single spring. The mechanisms having a single loop and single degree of freedom can be statically balanced by balancing each link with respect to the adjacent link and consequently no additional springs are needed to balance the out of plane mode.

Further work on the subject can include the synthesis and proof of the static balancing strategies found for the two reconfigurable mechanism groups.

## REFERENCES

- [1] Tseng, T.-Y., Hsu, W.-C., Lin, L.-F., and Kuo, C.-H., 2015. “Design and Experimental Evaluation of a Reconfigurable Gravity-Free Muscle Training Assistive Device for Lower-Limb Paralysis Patients”. In Proc. ASME 2015 Int. Des. Eng. Tech. Conf. Comput. Inf. Eng. Conf., ASME.
- [2] Kuo, C.-H., Dai, J. S., and Yan, H.-S., 2009. “Reconfiguration principles and strategies for reconfigurable mechanisms”. *2009 ASME/IFToMM Int. Conf. Reconfigurable Mech. Robot.*, pp. 1–7.
- [3] Slaboch, B. J., and Voglewede, P. a., 2014. “Profile Synthesis of Planar Rotational/Translational Variable Joints”. *J. Mech. Robot.*, **6**(4), p. 041012.
- [4] Wohlhart, K., 1996. “Kinematotropic Linkages”. In *Recent Adv. Robot Kinemat.* Springer Netherlands, ch. 7, pp. 359–368.
- [5] Dai, J. S., and Rees Jones, J., 1999. “Mobility in Metamorphic Mechanisms of Foldable / Erectable Kinds”. *ASME J. Mech. Des.*, **121**, pp. 375–382.
- [6] Nathan, R. H., 1985. “A Constant Force Generation Mechanism”. *ASME J. Mech. Transm. Autom. Des.*, **107**(4), pp. 508–512.
- [7] Gogu, G., 2009. Branching singularities in kinematotropic parallel mechanisms.
- [8] Yan, H.-S., and Kuo, C.-H., 2009. “Structural Analysis and Configuration Synthesis of Mechanisms with Variable Topologies”. In ASME/IFToMM Int. Conf. Reconfigurable Mech. Robot., IEEE, pp. 23–31.
- [9] Gao, D. Z., Cai, G. W., Shi, H., and Pan, Y. C., 2013. “Adjacency Matrix Based Analysis on a Novel Metamorphic Manual Operation Sugarcane Loader”. *Appl. Mech. Mater.*, **397-400**, pp. 1529–1533.
- [10] Kong, X., and Pflurner, M., 2015. “Type synthesis and reconfiguration analysis of a class of variable-DOF single-loop mechanisms”. *Mech. Mach. Theory*, **85**, pp. 116–128.
- [11] Galletti, C., and Fanghella, P., 2001. “Single-loop kinematotropic mechanisms”. *Mech. Mach. Theory*, **36**(6), pp. 743–761.
- [12] Kong, X., and Huang, C., 2009. “Type synthesis of single-DOF single-loop mechanisms with two operation modes”. In 2009 ASME/IFToMM Int. Conf. Reconfigurable Mech. Robot., ASME/IFToMM, pp. 136–141.
- [13] Hao, G., Kong, X., and He, X., 2014. “A planar reconfigurable linear rigid-body motion linkage with two operation modes”. *Proc. Inst. Mech. Eng. Part C J. Mech. Eng. Sci.*, **228**(16), pp. 2985–2991.
- [14] Kong, X., Gosselin, C. M., and Richard, P.-L., 2007. “Type Synthesis of Parallel Mechanisms With Multiple Operation Modes”. *J. Mech. Des.*, **129**(6), p. 595.
- [15] Muller, A., 2009. “On the Concept of Mobility Used in Robotics”. In Proc. IDETC/CIE, ASME, pp. 1275–1284.
- [16] Song, C., Chen, Y., and Chen, I.-M., 2013. “A 6R linkage reconfigurable between the line-symmetric Bricard linkage and the Bennett linkage”. *Mech. Mach. Theory*, **70**, pp. 278–292.
- [17] Balli, S. S., and Chand, S., 2004. “Synthesis of a Five-Bar Mechanism of Variable Topology Type With Transmission Angle Control”. *ASME J. Mech. Des.*, **126**(1), p. 128.
- [18] Ye, W., Fang, Y., and Guo, S., 2014. “Reconfigurable parallel mechanisms with planar five-bar metamorphic linkages”. *Sci. China Technol. Sci.*, **57**(1), pp. 210–218.
- [19] Fisher, R., Podhorodeski, R. P., and Nokleby, S. B., 2004. “Design of a reconfigurable planar parallel manipulator”. *J. Robot. Syst.*, **21**(12), pp. 665–675.
- [20] Palpacelli, M.-c., Carbonari, L., Palmieri, G., and Callegari, M., 2014. “Analysis and Design of a Reconfigurable 3-DoF Parallel Manipulator for Multimodal Tasks”. *IEEE/ASME Trans. Mechatronics*, **20**(4), pp. 1–11.
- [21] Zhang, K., Fang, Y., Wei, G., and Dai, J. S., 2012. “Structural Representation of Reconfigurable Linkages”. In *Adv. Reconfigurable Mech. Robot. 1*. Springer-Verlag, London, UK, pp. 127–137.
- [22] Gan, D., Dai, J. S., and Caldwell, D. G., 2011. “Constraint-Based Limb Synthesis and Mobility-Change-Aimed Mechanism Construction”. *ASME J. Mech. Des.*, **133**(5).
- [23] Zhang, L., and Dai, J. S., 2009. “Metamorphic techniques and geometric reconfiguration principles”. In 2009 ASME/IFToMM Int. Conf. Reconfigurable Mech. Robot., pp. 32–40.
- [24] Herder, J. L., 2001. “Energy-free systems: theory, conception, and design of statically balanced spring mechanisms”. PhD thesis, Delft University of Technology.
- [25] Streit, D. A., and Shin, E., 1993. “Equilibrators for Planar Linkages”. *J. Mech. Des.*, **115**(3), pp. 604–611.
- [26] Gosselin, C. M., and Wang, J., 1998. “On the design of gravity-compensated six-degree-of-freedom parallel mechanisms”. *Proceedings. 1998 IEEE Int. Conf. Robot. Autom.*, **3**(May), pp. 2287–2294.



## Preliminary Work

The static balancing solution presented in Paper 1 is the result of some conceptual development. The problem when starting the project was whether a reconfigurable mechanism with two, one DoF configurations could be balanced using a single spring. An initial literature search was performed to find other sources relating to the problem, during the search it was apparent that no other sources related to this problem and a solution had to be designed.

### A.1. Current Solution by Tseng

The mechanism by Tseng et al. [2] was balanced using two separate springs. This can be seen in the figure below.

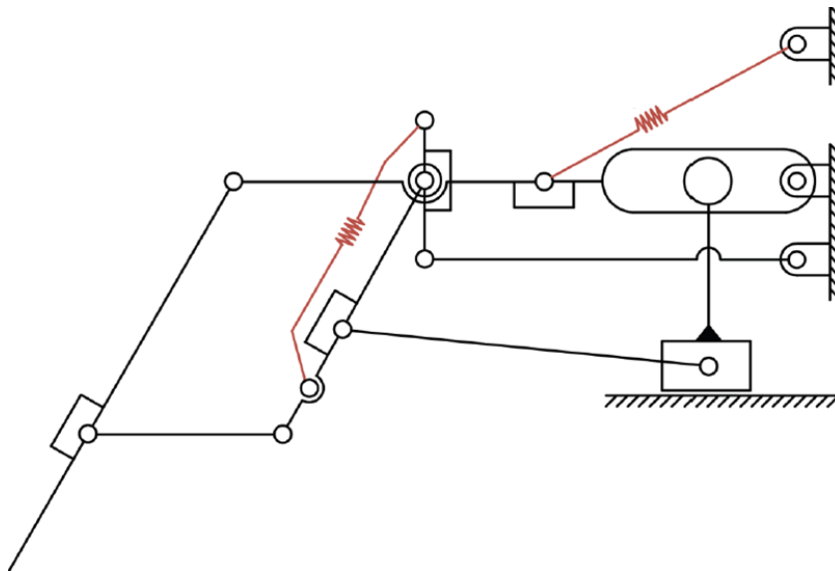


Figure A.1: Two-spring balanced mechanism by Tseng [2]

## A.2. Static balancing

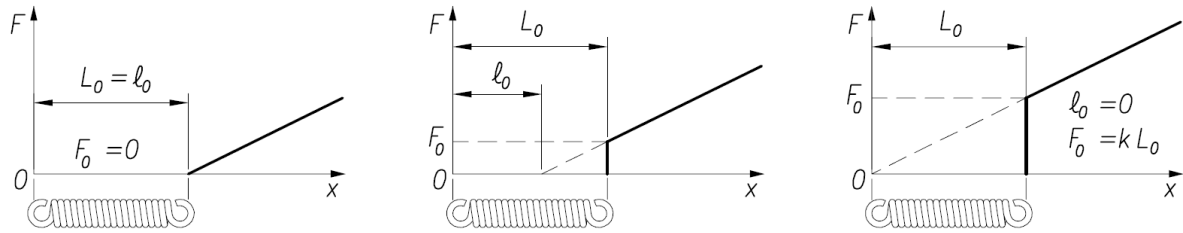


Figure A.2: Illustration of the free-length in springs [1]

To come to a suitable concept, the static balancing techniques had to be explored. Static balancing is a way to compensate the weight of a mass against gravity. Classical techniques for this include counterweights and even gas balloons can be used to compensate the weight of an object against gravity. In this paper, static balancing using springs is further explored.

The simplest form of static balancing using a spring is by using a zero free-length spring. In Fig. A.2 a figure illustration of free-length can be seen. By using zero free-length springs the force in the spring is proportionate to the length of the spring instead of the deflection.

The first sketches explored the different types of balancing and methods for spring placement. In Fig. ?? some of these initial sketches are shown.

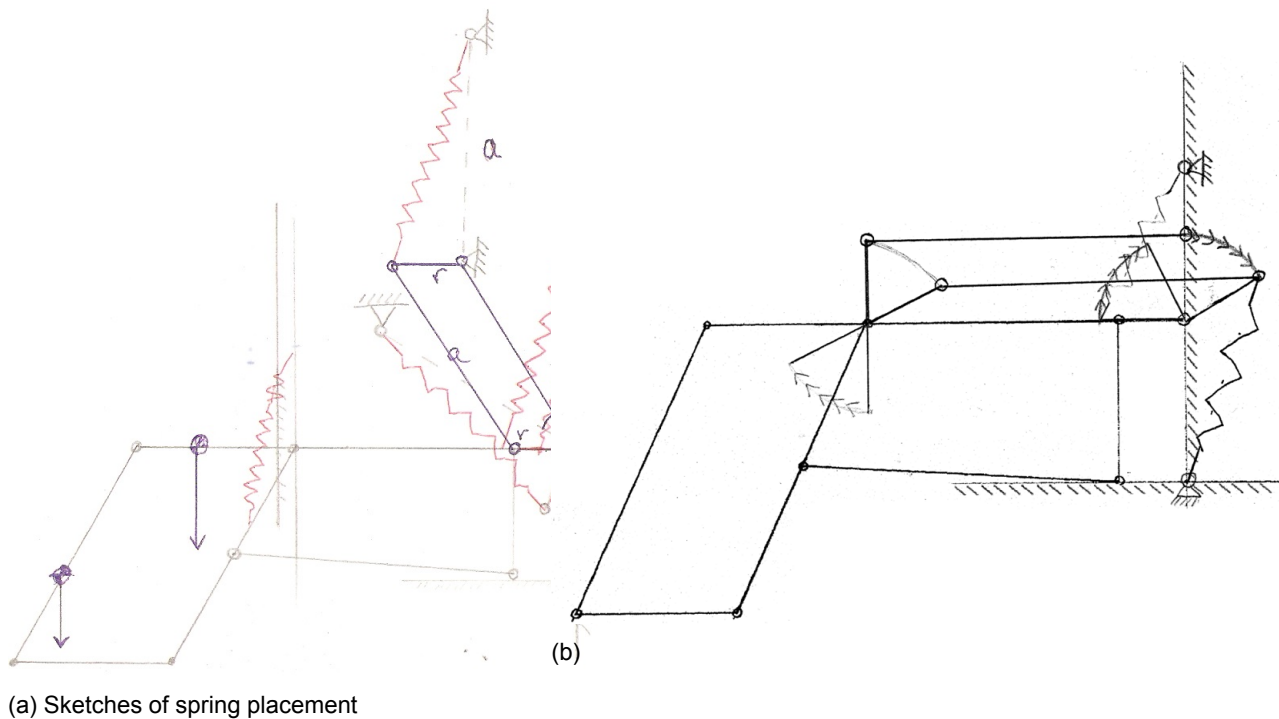


Figure A.3: Sketch of initial concept

### A.3. First concept

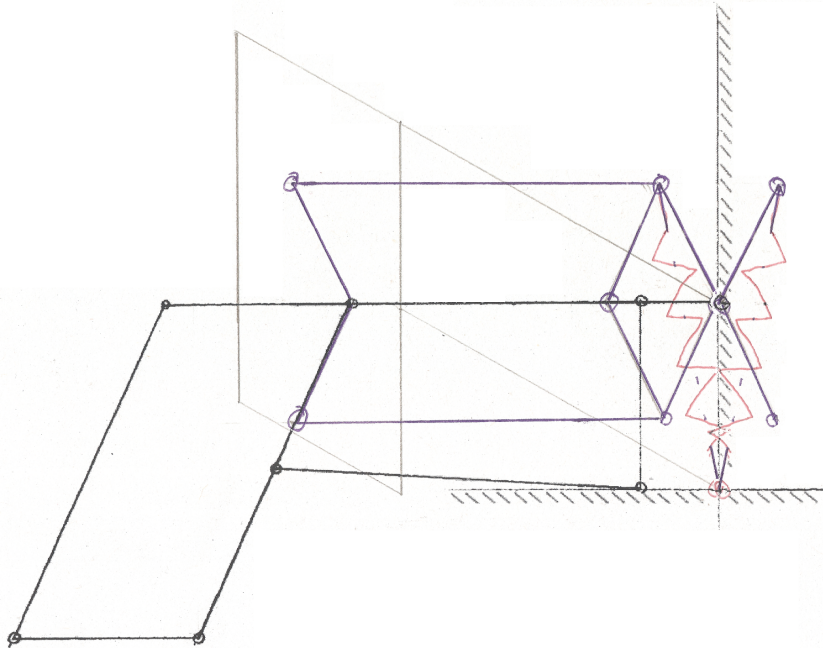


Figure A.4: First preliminary concept

Before the current solution, another concept was developed that also could have been successful. Instead of a cable and pulleys, this design relied on adding links and a zero free-length spring to achieve a static balance of the two configurations. What can be seen in Fig. A.4 is that a double parallelogram construction is used to shift the spring from the lower leg to near the origin. The spring would pull down on the left side to operate the lower leg motion and on the right of the origin for the upper leg motion.

This design was abandoned in an early concept stage so no further developments were made. The spring would be attached to an operating link that would swing from the left side to the right depending on the operation mode the patient would be in. The operating link would somehow have to detach itself from the double parallelogram and connect to the main horizontal link to balance the upper leg motion.

This concept was abandoned for a number of reasons. First, because the spring is mounted in line with the origin of the hinges, the spring would not balance the mechanism in the transition so the mechanism would have to rely on external constraints to prevent the mechanism from 'falling down'. Second the mechanism uses a lot of additional links adding to the complexity of the mechanism. And third the mechanism depends on a zero free-length spring that would require an expensive spring or additional measures to compensate for the free-length of a normal spring.



# B

## ADAMS

The first step of the validation of the theories was the performing of a simulation. This simulation was done in ADAMS, this is a multi-body dynamics software that could provide a completely different way of demonstrating the working of the mechanism. In this appendix the different elements to the ADAMS simulations are explained.

### B.1. ADAMS Build details

The model is made using simple links that are connected either to each other or to the ground using certain joints. Mostly these are revolute joints but in two instances these are slider joints. The mechanism can be seen in Fig. B.1.

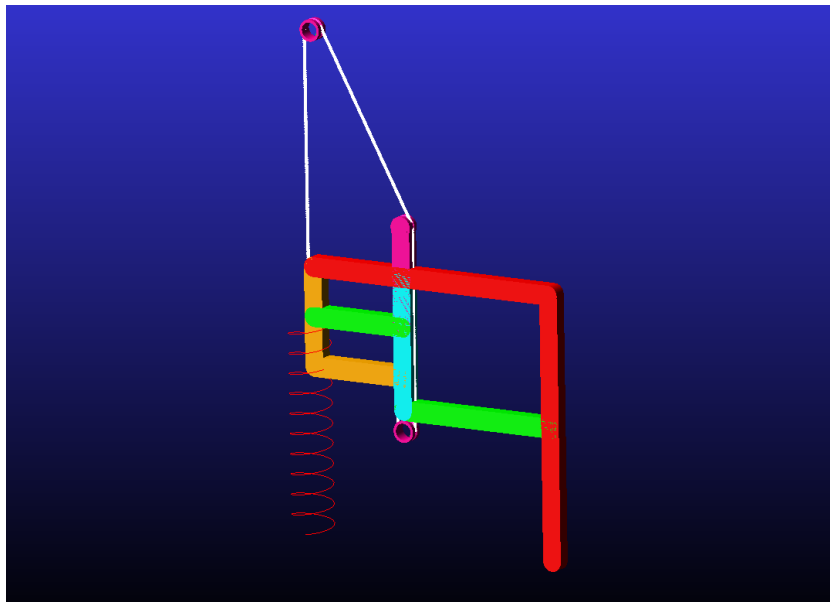


Figure B.1: Render of the model in ADAMS

For clarity, below is the image of the mechanism with the link numbers.

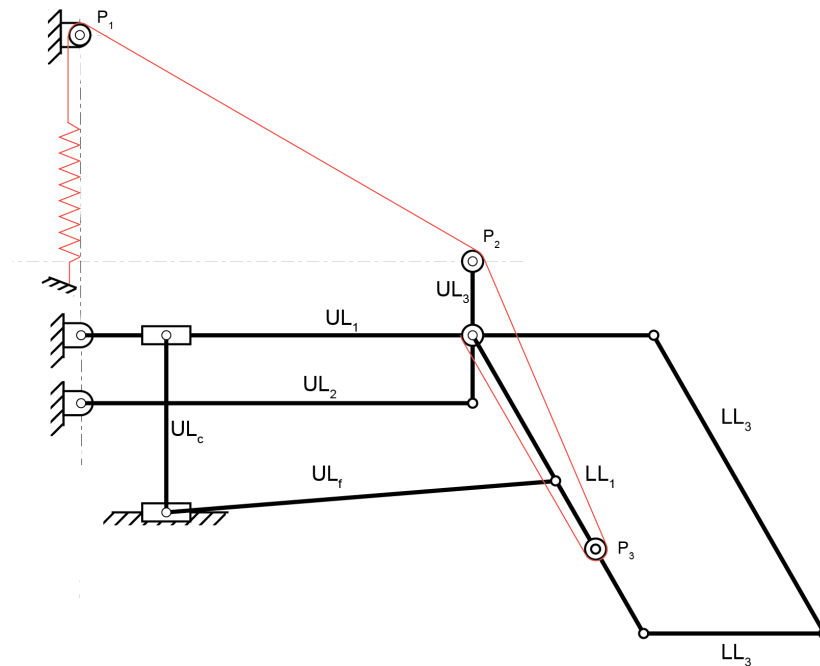


Figure B.2: Mechanism with link numbers

### B.1.1. Spring calculations

To find the correct dimensions of the spring connection and the correct spring constant. Matlab was used to calculate the right proportion of the dimensions. The spring constant is first calculated for each configuration and then the parameters were found by iteration.

```

1  g = 9.80665; %Gravity in ADAMS
2
3  % Masses of the mechanism and pulleys
4  Mul1=2;
5  Mul2=0.8;
6  Mul3=0.8;
7  Msli=0.8;
8  Mfol=0.8;
9  Ml11=1;
10 Ml12=2;
11 Ml13=1.3;
12 Mp1=1;
13 Mp2=1;
14 Mp3=1;
15 Mp4=1;
16
17 % Locations of the centres of mass
18 Lul1=0.4;
19 Lul2=0.15;
20 Lul3=0.15;
21 Lsli=0.15;
22 Lfol=0.15;
23 Ll11=0.2;
24 Ll12=0.4;
25 Ll13=0.25;
26
27 % Parameters of the spring connections
28 a1 = 0.26403
29 r1 = 0.15;
30
31 a2 = 0.0750;
32 r2 = 0.23162922;
33

```

```

34 a1a = 0.475+a1
35 r2a=0.4-r2
36
37 % Calculation of the spring constants in each mode
38 k1 = (Mul1*0.5*Lul1+Mul2*0.5*Lul2+Mul3*r1+Mfol*0.5*Lfol+Ml11*r1+Ml12*Lul1+Ml13*0.5*r1+ ...
...
39 Ml13*0.5*Lul1+(Mp2+Mp3+Mp4)*r1)*g/(a1*r1)
40 k2 = (Ml11*0.5*Ll11+Ml13*Ll11+Ml12*0.5*Ll12+Mp3*r2+0.5*Mfol*0.15)*g/(a2*r2)
41
42 % Calculation of the cable force
43 Fz = (Mul1*0.5*Lul1+Mul2*0.5*Lul2+Mul3*r1+Mfol*0.5*Lfol+Ml11*r1+Ml12*Lul1+Ml13*0.5*r1+...
44 Ml13*0.5*Lul1+(Mp2+Mp3+Mp4)*r1)*g*sqrt(a1^2+r1^2)/(r1*a1);
45
46 % Determining the spring length of the mechanism
47 lv = Fz/k1
48 lv_calc=sqrt(a1^2+r1^2);
49 FV_calc = k1*lv_calc

```

The results from these calculations were the spring constant needed but also the location of the pulleys and the pre-load of the spring.

parameters		
$a_1$	0.264	[m]
$r_1$	0.15	[m]
$a_2$	0.0750	[m]
$r_2$	0.232	[m]
$k$	593.6	[N/m]
<i>preload</i>	180.27	[N]

Table B.1: Parameters from the Matlab calculation

## B.1.2. Cable Toolbox

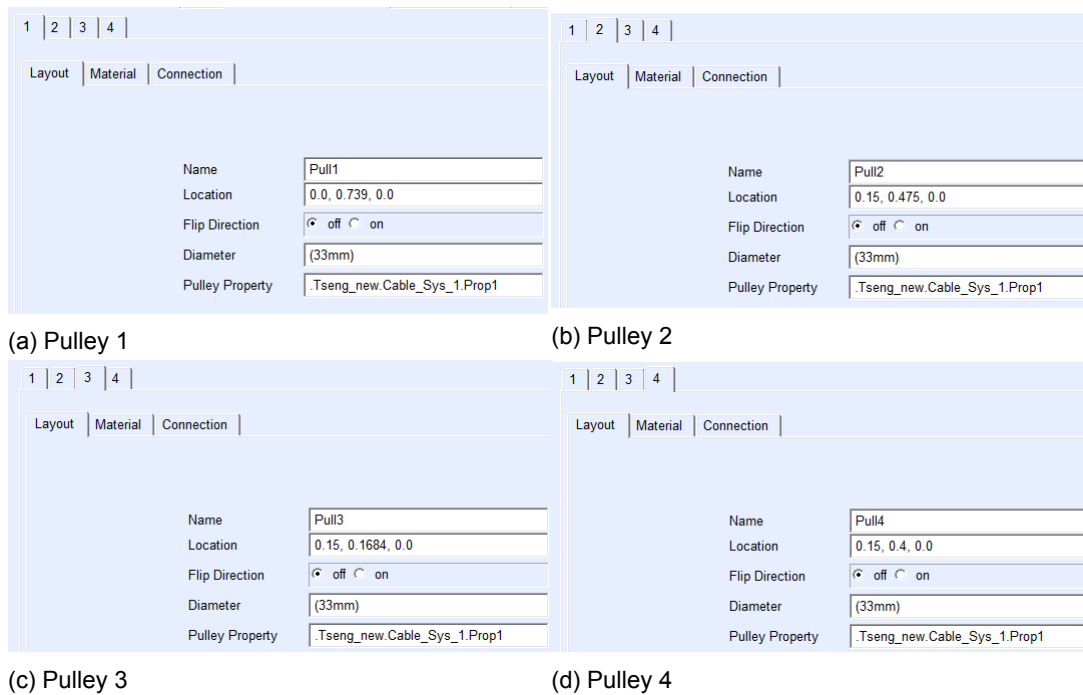


Figure B.3: Location of the pulleys

The cable and pulleys are implemented using the cable toolbox in the software. The cable parameters can be seen below in Fig. B.4. This toolbox generates a large number of smaller parts with certain interactions based on the input parameters provided. One of these is the thickness of the cable and the Young's modulus. These are set to be very high because the strain in the cable will otherwise be extremely large. When using the parameters as set in fig. B.4, measurements were performed to check the strain on the cable, these were found to be in the order of  $10^{-6}m$ , so they were not significant.

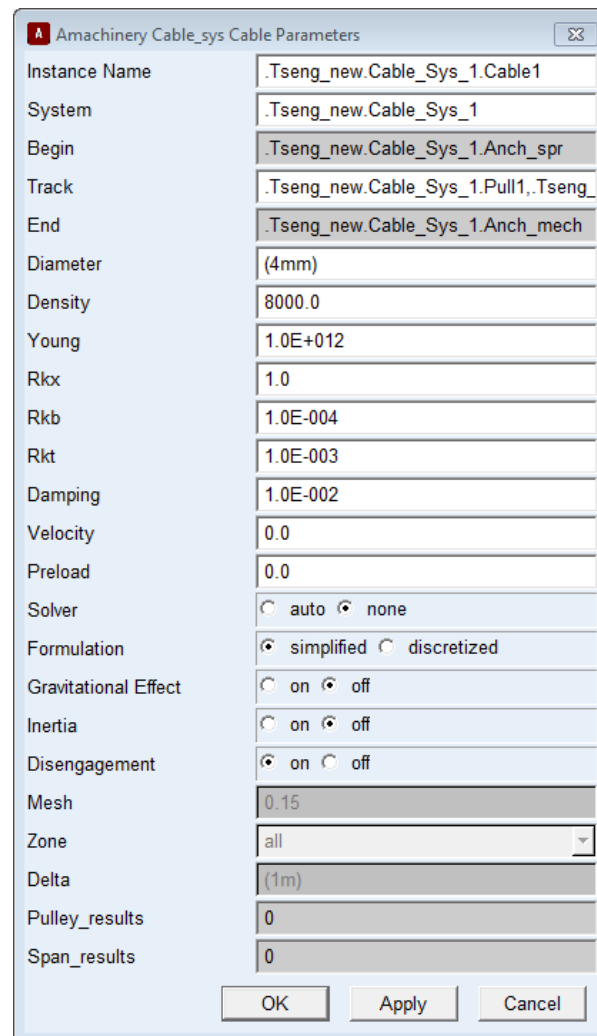


Figure B.4: Cable settings

The cable was attached to the spring by means of a small 'box' part with a mass of  $0.001g$ , the influence of this on the mechanism was measured but the potential energy increase of this can be neglected.

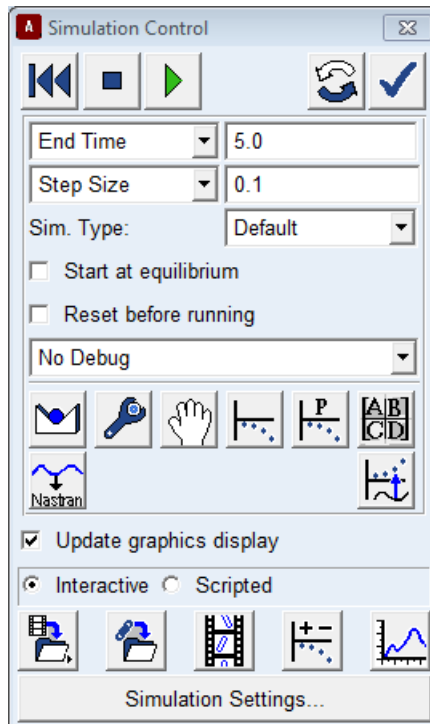
### B.1.3. Motions

Two motions are active on the mechanism. These sequentially operate the configurations of the mechanism. These are a rotation motion for the first configuration and a linear motion for the second joint. The linear motion is chosen because no other connection between ground and the lower configuration links can be made. Both motions are based on two STEP functions, the first configuration having a displacement of 15 degrees, the second configuration having a displacement of  $8cm$ .

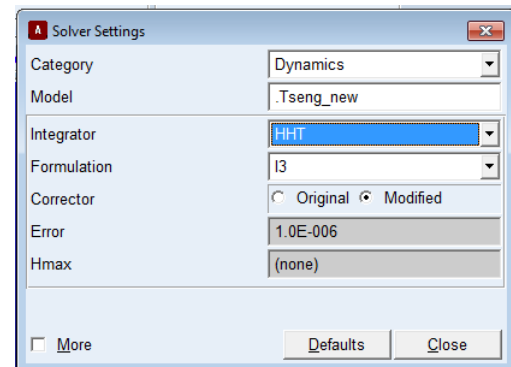
### B.1.4. Solver settings

In the simulation settings in Fig. B.5 the simulation settings can be found. Each motion of the configuration runs for four seconds, this is to prevent that dynamic forces would be present on the mechanism.

In Fig. B.5b the integrator settings are found. An HHT integrator is used with an error of  $10^{-6}$  this relatively accurate setting is needed because of the singularity position of the mechanism. When a larger error is chosen, the simulation runs a lot quicker but will often seize because of a wrong path being chosen from the singularity position.



(a) Simulation settings



(b) Integrator settings

Figure B.5: Settings of the Simulation Control

## B.2. Full ADAMS Results

In Fig. B.6 the total potential energy can be seen. We can see that the potential energy is not completely a flat line. There is a variation of about  $0.015 \text{ J}$ . This variation means that either the gravitational potential energy is higher or, more likely, the spring does not contract enough.

What we can learn from this plot is that there are no 'jumps' in potential energy from the first to the second configuration. Which is the most important criteria that had to be fulfilled.

The most likely cause of the peaks in the potential energy plots can be due to the width of the cable. The cable used is  $2 \text{ mm}$  wide. In the plot shown in Fig. B.7 we can see a virtually flat line. This line is obtained by slightly increasing the height of the pulleys by  $1 \text{ mm}$ . This however remains speculation because this cannot be incorporated into the equations calculating the dimensions of the mechanism.

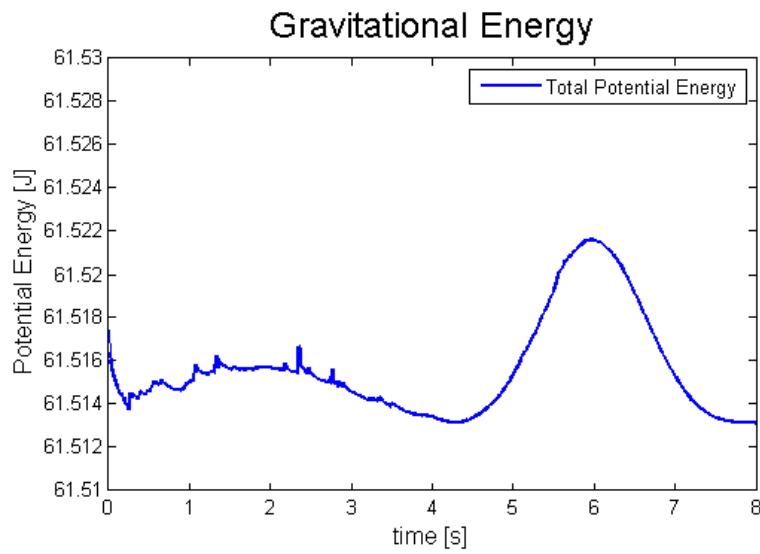
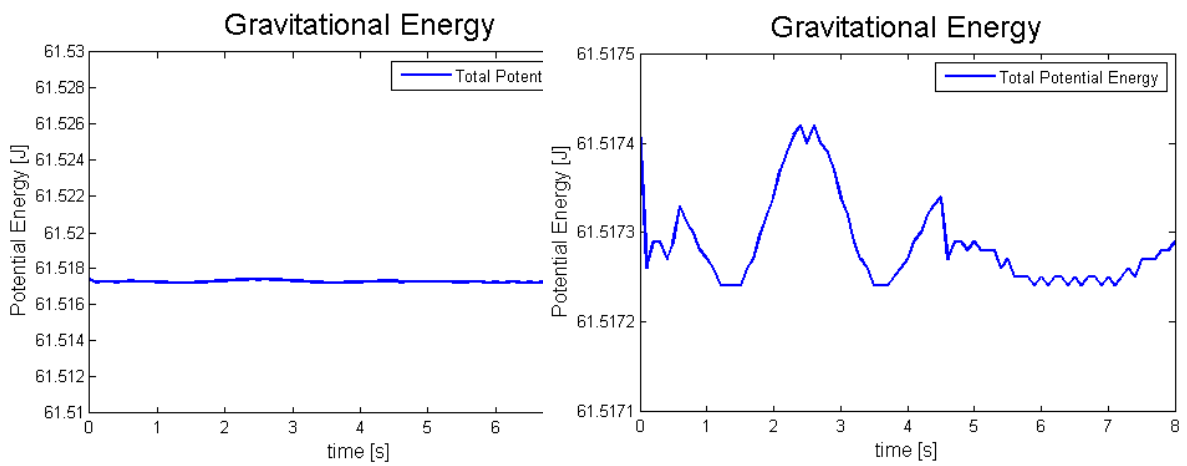


Figure B.6: Plot of the total potential energy

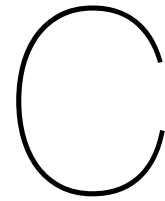


(a) Adjusted axes

(b) Unadjusted axes

Figure B.7: Plot of the total potential energy with iterated pulley position





# Physical Model

## C.1. Details of the physical model

In this section the calculations for the selection of a suitable spring are made. Just like in the actual model the mass of the links and additional mass of the patients' leg are taken into account for spring selection. In this case however, no patient will be testing the device so we can choose additional masses convenient for the selection of a spring. The masses in the physical model are sections of round steel bar connected to the mechanism using M5 thread.

mass	[kg]
mUL1	0.0527
mULv	0.0088
mUL2	0.012
mUL3	0.0103
mULf	0.012
mLL1	0.0081
mLL2	0.016
mLL3	0.0195
mP	0.002
mP2	0.0073

Table C.1: Masses of the links and body

Link	Configuration 1	Configuration 2 [m]
UL1	0.1	
UL2	0.075	
UL3	0.0375	
ULf	0.0375	
ULc	0.05	
LL1	0.075	0.01875
LL2	0.2	0.035
LL3	0.1375	0.03750
P1	0.075	
P2	0.075	0.050
P3	0.075	
c1mE1	0.15	
c2mE2	0.075	0.06

Table C.2: Position of centres of mass on the mechanism

This data is then used for the correct spring calculation in matlab:

```

1  clc
2
3  g = 9.812;
4
5  mUL1 = 0.0527;
6  mULv = 0.0088;
7  mUL2 = 0.012;
8  mUL3 = 0.0103;
9  mULf = 0.012;
10 mLL1 = 0.0081;
11 mLL2 = 0.016;
12 mLL3 = 0.0195;
13 mP   = 0.002;
14 mP2  = 0.0073;
15 mE1  = 0.212;
16 mE2  = 0.226;
17
18 c1UL1 = 0.1;
19 c1UL2 = 0.075;
20 c1UL3 = 0.0375;
21 c1ULf = 0.0375;
22 c2ULf = 0.05;
23 c1LL1 = 0.075;
24 c2LL1 = 0.01875;
25 c1LL2 = 0.2;
26 c2LL2 = 0.035;
27 c1LL3 = 0.1375;
28 c2LL3 = 0.03750;
29 c1P1  = 0.075;
30 c1P2  = 0.075;
31 c2P2  = 0.050;
32 c1P3  = 0.075;
33 c1mE1 = 0.15;
34 c2mE2 = 0.06;
35
36 %a1 = 0.2250;
37 a1 = 0.15;
38 r1 = 0.075;
39
40 a2 = 0.0375;
41 r2 = 0.05;
42
43 %
44 %
45
46
47 a1a = 0.475+a1
48 r2a=0.4-r2
49
50 k1 = (mUL1*c1UL1+mUL2*c1UL2+mUL3*c1UL3+mULf*c1ULf+mLL1*c1LL1+mLL2*c1LL2+mLL3*c1LL3+...
51 3*mP*c1P1+mP2*c1LL2+mE1*c1mE1+mE2*c1LL2)*g/(a1*r1)
52 k2 = (mULf/2*c2ULf+mLL1*c2LL1+mLL2*c2LL2+mLL3*c2LL3+mP*c2P2+mE2*c2mE2)*g/(a2*r2)
53
54 knm = k1/1000
55
56
57 %density steel is 8.05 g/cm3
58
59 (340/8.05)/(pi*1.5^2);
60 (300/8.05)/(pi*1.5^2);
61
62 (100/8.05)/(5);
63
64 % Calculation of gravitational force
65 Fz = (Mul1*0.5*Lul1+Mul2*0.5*Lul2+Mul3*r1+Mfol*0.5*Lfol+Mll1*r1+Mll2*Lul1+...
66 Mll3*0.5*r1+Mll3*0.5*Lul1+(Mp2+Mp3+Mp4)*r1)*g*sqrt(a1^2+r1^2)/(r1*a1);
67
68 lv = Fz/k1
69 lv_calc=sqrt(a1^2+r1^2);
70 FV_calc = k1*lv_calc

```

These calculations lead to the following parameters:

$a_1$	0.15	m
$r_1$	0.075	m
$a_2$	0.0375	m
$r_2$	0.05	m
k	81	N/m

Table C.3: Masses of the links and body

## C.2. Physical model Solidworks Design

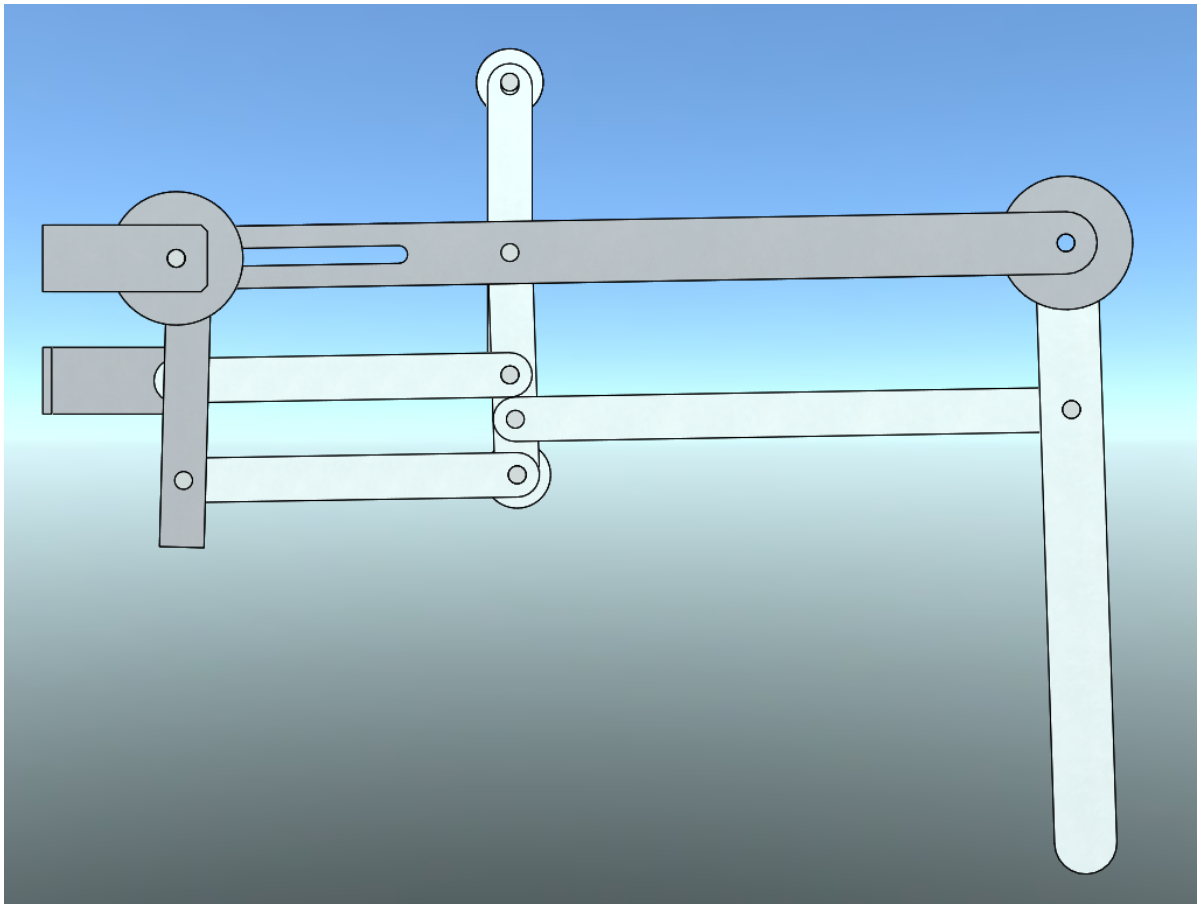


Figure C.1: Rendering of the side of the mechanism (without spring)

Figure C.1 shows a render of the side of the mechanism. The dark elements are made of aluminium, the lighter elements of steel. The aluminium parts are made of this material because they had to be machined. Especially the upper leg link was crucial as this part created the constraint that would make sure the two configurations were not able to operate simultaneously. This part is shown in Fig. . To keep the mechanism simple, the rest of the parts are made of *2mm* steel that was cut using a laser cutter.

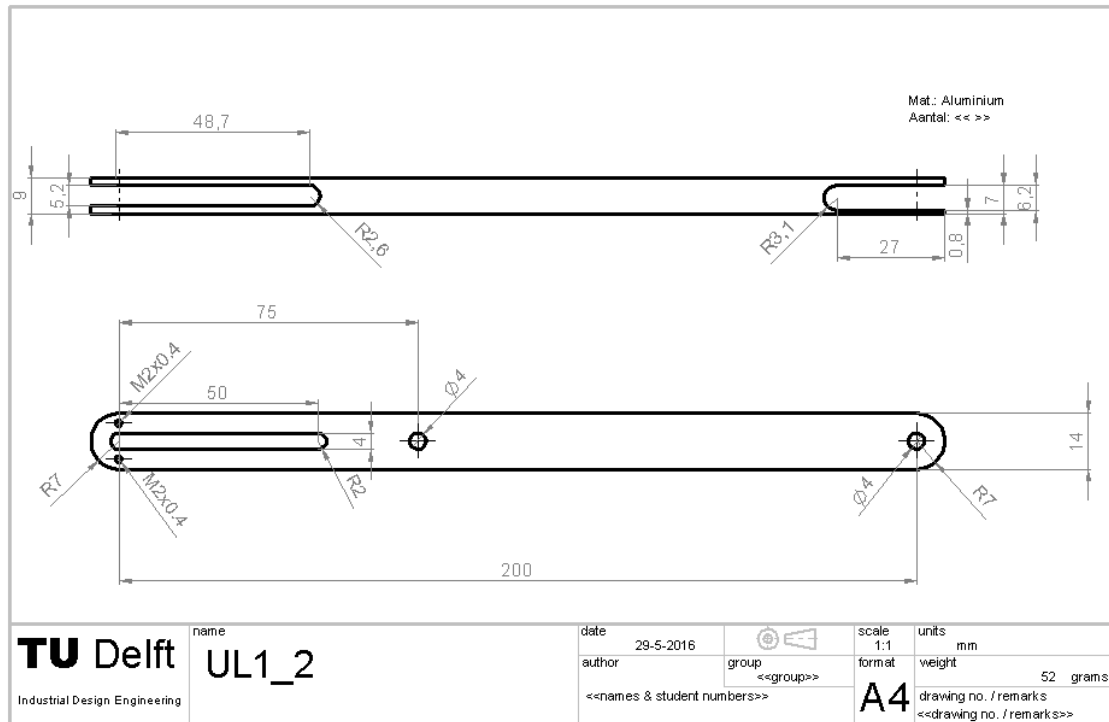


Figure C.2: Drawing of upper leg link UL1

### C.3. Experiment Design

The experiment was performed on a Zwick Universal Testing Machine. In Fig. C.3 the testing machine can be seen. The machine works in a vertical plane so an extra bearing is needed to lead the cable from the mechanisms. The cable is used to actuate both configurations of the mechanisms. One 1mm steel cable is used for each configuration. The mechanism is mounted on a aluminium base plate, in the following section we will learn that this should have been made using a thicker material. The cables are connected to a disc one on the upper-leg and one on the lower-leg link.

For the sliding joint a linear bearing is used. The other sliding joint, along the upper-leg link a axle in a slot in the link. This joint was a major cause of friction. This could have been reduced by using a bearing on the axle or by also using an aluminium axle to there is no difference in hardness of the materials.

The mechanism has no bearings because this was not deemed necessary to provide a proof of principle of single spring balancing. From the conclusions in Paper 1 we now know that this was indeed the case and a sufficient graph was produced. However a more exact graph, that would have followed the behaviour of the ADAMS model could have been produced if a mechanism with less friction had been made.

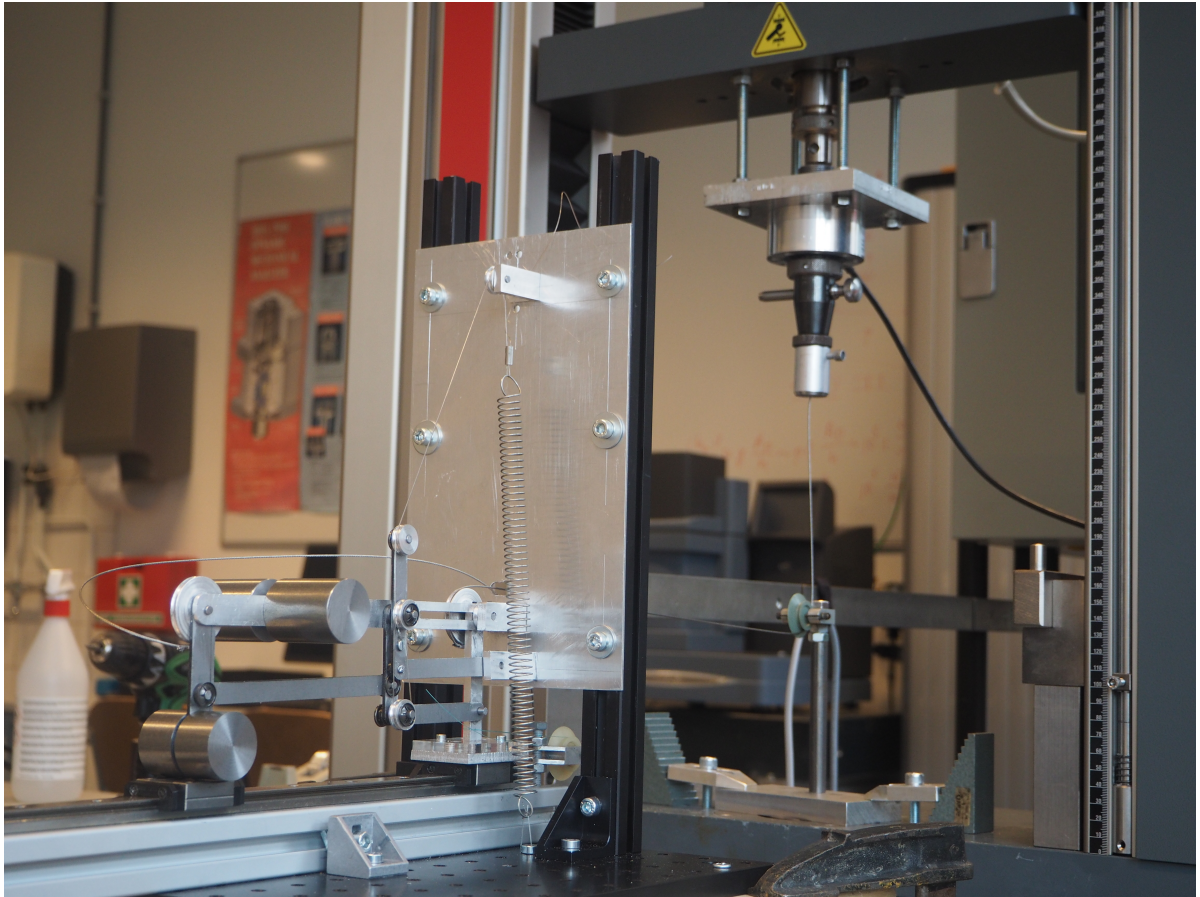
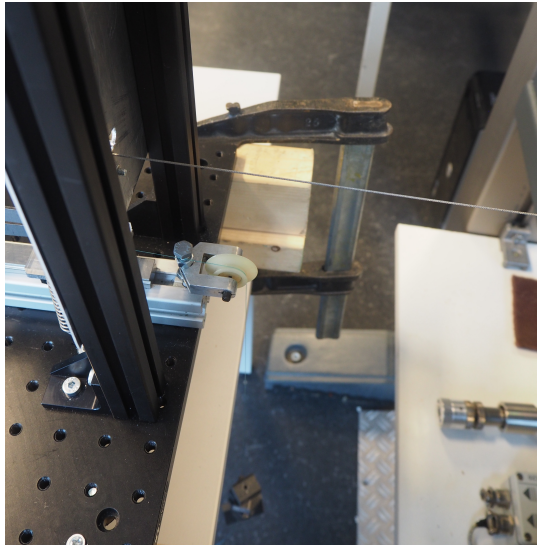


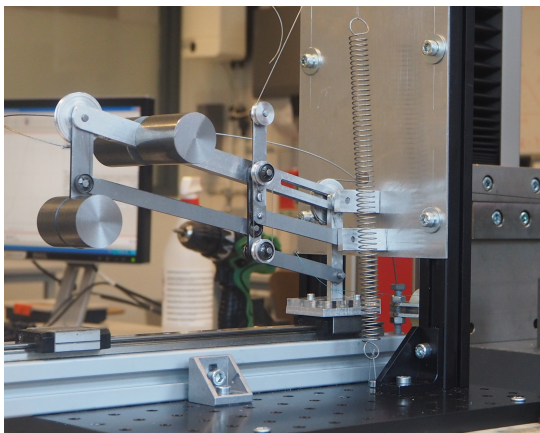
Figure C.3: Photograph of experimental set-up



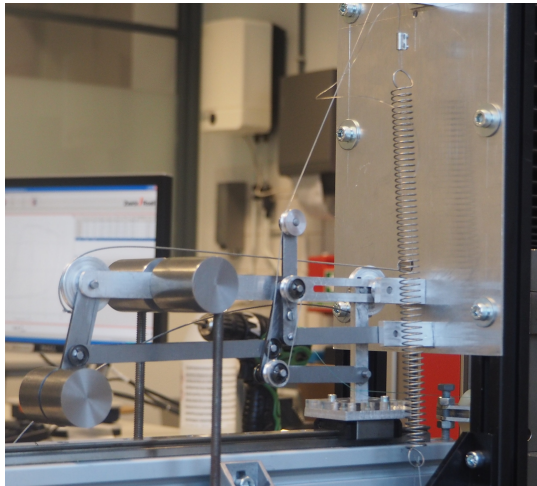
(a) Cable along additional bearing



(b) Additional weights for configuration 2



(c) Operation of configuration 1

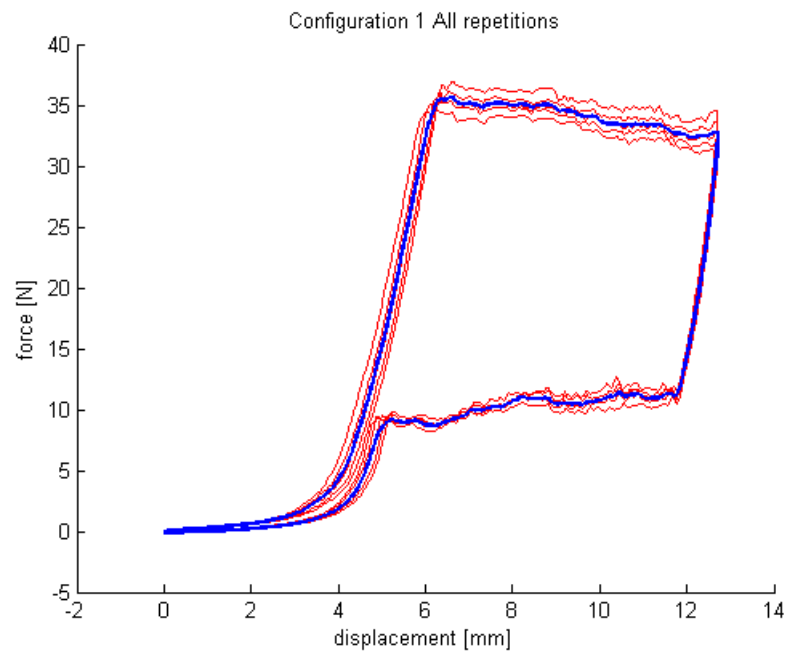


(d) Operation of configuration 2

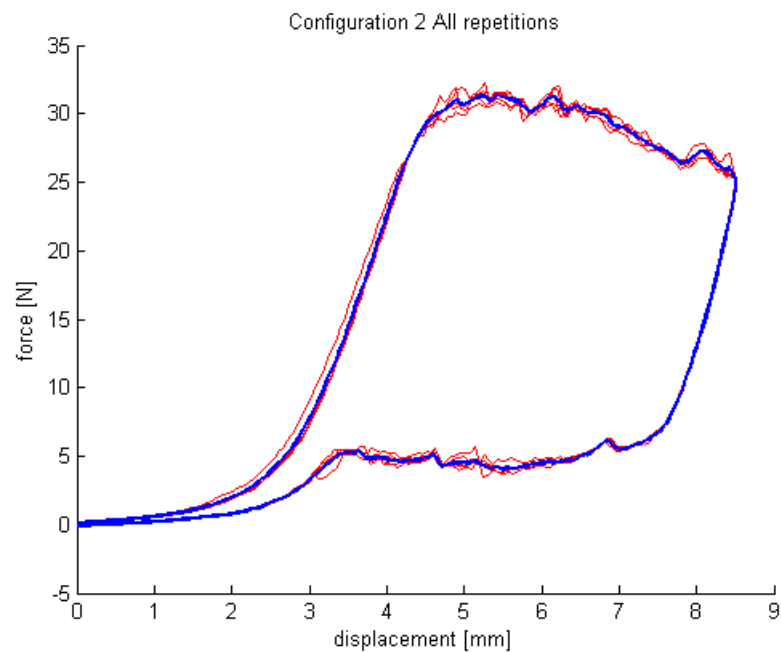
Figure C.4: Photo's of the experimental set-up

## C.4. Full test results

The experiment was repeated five times per configuration. The average of each configuration was taken for all the repetitions. This lead to the following plots in Fig. C.5.



(a) Average of configuration 1



(b) Average of configuration 2

Figure C.5: Hysteresis loops of the configurations

These plots include the additional force that was added for the mechanism to realise a loop. To find whether both configurations are statically balanced, this additional weight has to be subtracted from the data in the plot. The additional mass for configuration 1 is added to link 4 and for configuration 2 is added to link 9, (which is transferred through link 2 to link 6). This means that the additional moment

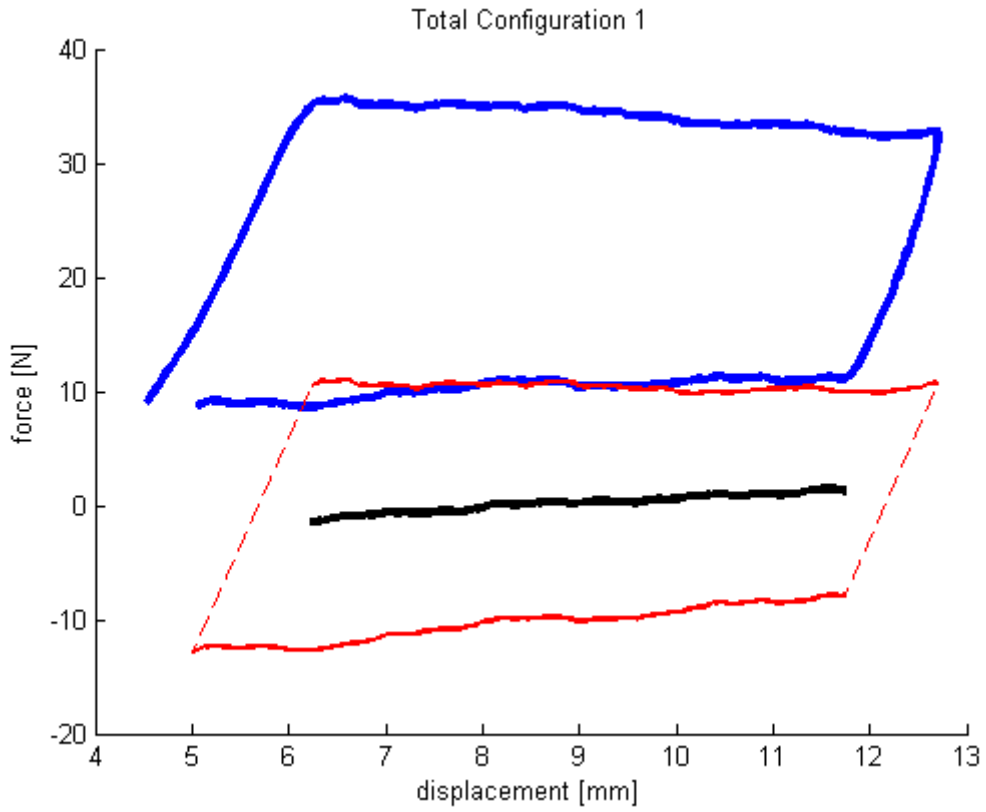
due to each weight for both configurations decreases by the cosine of the mechanism angle. The mechanism is then statically balanced if the average of the loop is zero, after the weight has been subtracted.

In Fig. C.5 a slope on the left and right side of the graph can be seen. Ideally these would be vertical lines as that would show that only static friction has to be overcome before the mechanism starts to move. The slope means that there is some flex in the mechanism. The most probable cause for this is the base plate to which the mechanism is attached, but this is not proved by creating a stiffer plate.

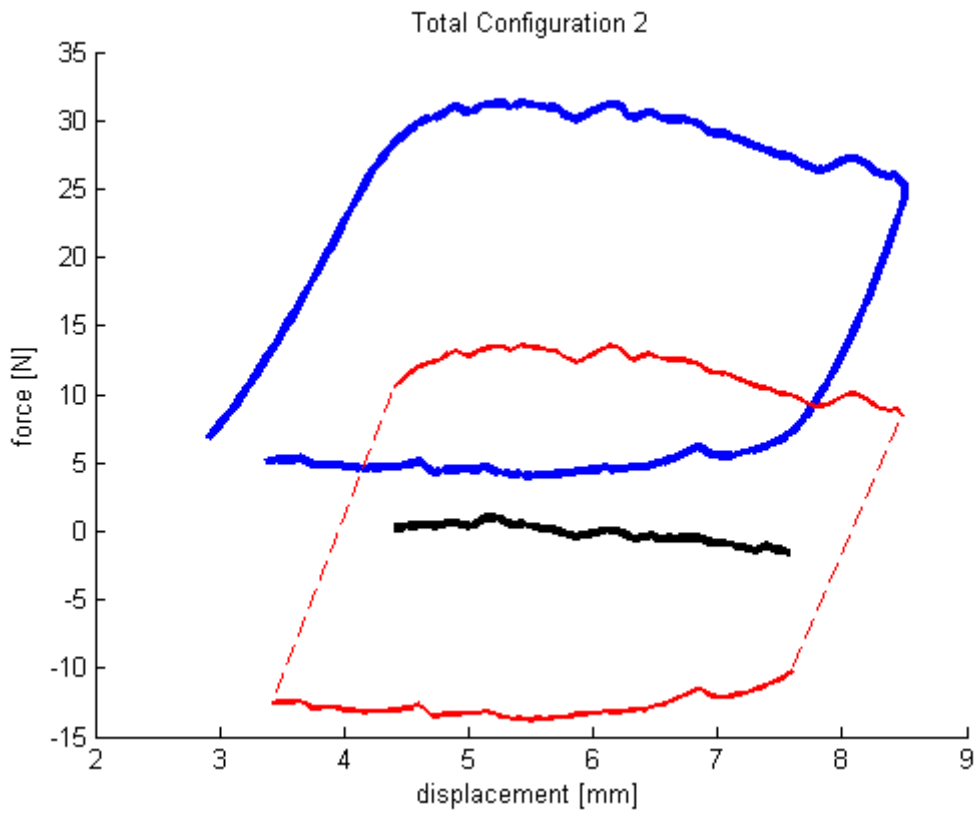
Both loops are split into an up and down motion because we can find the resting positions from the graph. This means that the angle of the mechanism can be more accurately determined from the graph, by taking the displacement for each motion. This enables the calculation of the angle of the mechanism which is needed to subtract the additional weight.

Because of the flexion in the mechanism, the up and down motion of the mechanism are not above each other, therefore the average is calculated over the remaining common path.

After subtraction and plotting of the average, the figures can be seen in Fig. C.6. The red lines represent the subtracted average. The black line the average of the up- and down motion. In both graphs a relatively flat line is seen around zero. This is the desired behaviour of a statically balanced mechanism.



(a) Configuration 1



(b) Configuration 2

Figure C.6: Plots adjusted for weight and average of each path

## C.5. Test Result Processing

```

1 %% Importing data from measurements
2
3 Dc1(1) = importdata('hefboomtensile11.txt');
4 Dc1(2) = importdata('hefboomtensile12.txt');
5 Dc1(3) = importdata('hefboomtensile13.txt');
6 Dc1(4) = importdata('hefboomtensile14.txt');
7 Dc1(5) = importdata('hefboomtensile15.txt');
8 Dc2(1) = importdata('hefboomtensile16.txt');
9 Dc2(2) = importdata('hefboomtensile17.txt');
10 Dc2(3) = importdata('hefboomtensile18.txt');
11 Dc2(4) = importdata('hefboomtensile19.txt');
12 Dc2(5) = importdata('hefboomtensile20.txt');
13
14 %%
15
16 % Additional weight per mode
17 EWc1 = 9.812*(446-212)/1000;
18 EWc2 = 9.812*(508/1000);
19
20 % Creating same size matrices by removing end data
21 Dc1_avg(:,:,1) = Dc1(1).data(8:497,1:3);
22 Dc1_avg(:,:,2) = Dc1(2).data(8:497,1:3);
23 Dc1_avg(:,:,3) = Dc1(3).data(7:496,1:3);
24 Dc1_avg(:,:,4) = Dc1(4).data(8:497,1:3);
25 Dc1_avg(:,:,5) = Dc1(5).data(8:497,1:3);
26
27 % Creating average path
28 DC1_av = mean(Dc1_avg,3);
29
30 %% Configuration 1
31
32 % Split in to two movements
33 AV1_up = DC1_av(118:239,2:3);
34 AV1_down = DC1_av(260:386,2:3);
35
36 % Subtract additional moments from measured forces
37 AV1_up = [AV1_up ...
38           AV1_up(:,2)-cosd((AV1_up(:,1)-6.2498).*(360/(2*pi*14))))*EWc1*0.15/0.014];
39 AV1_down = [AV1_down ...
40            AV1_down(:,2)-cosd((AV1_down(:,1)-4.9957).*(360/(2*pi*14))))*EWc1*0.14/0.015];
41
42 % Creating average of common paths
43 AV1_lim(:,:,1) = AV1_down(1:104,1:3);
44 AV1_lim(:,:,2) = AV1_up(1:104,1:3);
45 AV1_lim(:,:,3) = mean(AV1_lim,3);
46
47 %% Configuration 2
48 DC2_1 = Dc2(1).data(8:340,1:3);
49 DC2_2 = Dc2(2).data(8:340,1:3);
50 DC2_3 = Dc2(3).data(8:340,1:3);
51 DC2_4 = Dc2(4).data(8:340,1:3);
52 DC2_5 = Dc2(5).data(8:340,1:3);
53
54 Dc2_avg(:,:,1) = DC2_1(:,2:3);
55 Dc2_avg(:,:,2) = DC2_2(:,2:3);
56 Dc2_avg(:,:,3) = DC2_3(:,2:3);
57 Dc2_avg(:,:,4) = DC2_4(:,2:3);
58 Dc2_avg(:,:,5) = DC2_5(:,2:3);
59
60 DC2_av = mean(Dc2_avg,3);
61
62 AV2_up = DC2_av(83:159,1:2);
63 AV2_down = [AV2_up ...
64             AV2_up(:,2)-cosd((AV2_up(:,1)-4.4131).*(360/(2*pi*14))))*EWc2*(0.05/0.014)];
65 AV2_down = DC2_av(180:258,1:2);

```

```
64 AV2_down = [AV2_down ...  
              AV2_down(:,2)-cosd((AV2_down(:,1)-4.9957).*(360/(2*pi*14)))*EWc2*(0.05/0.014)];  
65  
66 AV2_lim(:, :, 1) = AV2_down(1:60, 1:3);  
67 AV2_lim(:, :, 2) = AV2_up(1:60, 1:3);  
68 AV2_lim(:, :, 3) = mean(AV2_lim, 3);
```

# Bibliography

- [1] Just L Herder. *Energy-free systems: theory, conception, and design of statically balanced spring mechanisms*. PhD thesis, Delft University of Technology, 2001. URL <http://repository.tudelft.nl/view/ir/uuid:8c4240fb-0315-462a-8b3b-efbd0f0e68b6/>.
- [2] Tzu-Yu Tseng, Wei-Chun Hsu, Li-Fong Lin, and Chin-Hsing Kuo. Design and Experimental Evaluation of a Reconfigurable Gravity-Free Muscle Training Assistive Device for Lower-Limb Paralysis Patients. In *Proc. ASME 2015 Int. Des. Eng. Tech. Conf. Comput. Inf. Eng. Conf.*, Boston, Massachusetts, 2015. ASME. doi: DETC2015-46706.